

3

Particle size analysis by image analysis

3.1 Introduction

A microscope examination should always be carried out whenever a sample is prepared for particle size analysis. Such an examination allows an estimate of the particle size range of the powder under test and its degree of dispersion. If the dispersion is incomplete it can be determined whether this is due to the presence of agglomerates or aggregates and, if agglomeration is present, may indicate the need for an alternative dispersing procedure.

Microscopy is often used as an absolute method of particle size analysis since it is the only method in which the individual particles are observed and measured [1-3]. It is particularly useful in aerosol science where particles are often collected in a form suitable for subsequent optical examination. It is useful not only for particle size measurement but also for particle shape and texture evaluation, collectively called morphology, with sensitivity far greater than other techniques. Reports have also been presented of the use of microscopy to relate particle size to processing characteristics of valuable mineral ores [4,5]. Particle shape may be defined either qualitatively or quantitatively. The former includes the use of such terms as acicularity, roundness and so on. The latter, more definitively, compares perpendicularly oriented diameters, for example, to obtain shape factors. The introduction of automatic image analyzers allows for the determination of complex shape factors which were previously unobtainable. These factors are of great value in defining crystal morphology and relating this to operating (attrition during conveying, compaction and so on) and end-use properties.

A size analysis by number is simpler to perform than an analysis by mass since, in the former, the statistical reliability depends solely on the number of particles measured. For a mass analysis the omission of a single 10 μm particle leads to the same error as the omission of a thousand 1 μm

particles since they both have the same volume. For a particle size analysis by mass, 25 particles in the largest size category have to be counted, in order to obtain an estimated standard error of less than 2%. If all the particles in this area were counted the final count would run into millions. It is obvious therefore that the area to be examined must decrease with decreasing particle size and the results obtained must be presented as particles per unit area.

The problem may be likened to determining the size distribution of a number of differently sized homogeneous balls in a container. If the balls are of size 2, $2\sqrt{2}$, 4, $4\sqrt{2}$64, $64\sqrt{2}$, in line with the size ratios often adopted in optical microscopy, and the relative frequency of the top size category is found to be 8 in 1000 particles this can be readily converted to a mass frequency when the number of balls in the other size categories is known. If the estimated mass of the 25 particles is 10% of the sample then the forecasted percentage standard error is $(10/\sqrt{25})$ i.e. 2%. If, on completing the analysis, the mass percentage of the coarsest fraction is greater than 10% then it is necessary to count more coarse particles in order to maintain this level of accuracy.

The errors in converting from a number to a volume (mass) distribution are greatest when the size range is wide. For a narrowly classified powder, ranging in size from say 10 to 30 μm , it is necessary to use an arithmetic grading of sizes, probably a 2 μm interval in this case, but the same rules still apply and the direct conversion of a number distribution to a weight distribution can still give rise to considerable error at the coarse end of the size distribution. Using closer size intervals adds little to analytical accuracy but can greatly increase the computation time.

The images may be viewed directly or by projection. Binocular eyepieces are preferred for particle examination but monoculars for carrying out a particle size analysis since, by using a single eyepiece, the tube length can be varied to give stepwise magnification. Most experienced operators prefer direct viewing but projection viewing, less tiring to the eye, is often used for prolonged counting. Projection may be front or back. With the former the operation is carried out in a darkened room due to the poor contrast attainable. Back projection gives better illumination but image definition is poor; this can be rectified by using a system whereby two ground-glass screens are placed with their faces in contact and one is moved slowly relative to the other [6].

Some automatic counting and sizing devices work from photographic negatives or positives. The principle objection that can be leveled against photographic methods is that only particles in focus can be measured accurately and this can lead to serious bias. Although photographic

methods are often convenient and provide a permanent record, the processing time may well offset any advantage obtained. This is particularly true when a weight count is required since, from statistical considerations, a large number of fields of view are required for accurate results.

Light microscopy is best suited for the size range 0.8 to 150 μm , with a resolution of around 0.2 μm depending on the wavelength of the light source. Scanning electron microscopy (SEM) operates in the size range from 0.1 μm to 1000 μm with a resolution of 10 nm and transmission electron microscopy (TEM) from 0.01 μm to 10 μm with a resolution of 5 nm. Back scattered electrons and x-rays contain information on the chemistry and average atomic number of the material under the beam.

Groen *et al.* [7] determined the optimum procedure for automatic focusing of a microscope. Kenny [8] examined the errors associated with detecting the edge of the particle image and outlined a technique, suitable for automatic image analysis for minimizing this error.

The shape and texture of construction aggregates are important parameters that have a direct bearing on the strength and durability of their asphalt and concrete end products. Typically, a batch of material is rejected if more than a specific fraction of particles have elongation and flatness ratio that exceed some limit. In the ASTM procedure [9] the measurements are carried out on 100 particles using specially designed calipers. More recently this has been replaced by image analysis which reduces the measurement time to less than 10 minutes [10]. In addition, this procedure is capable of conducting other useful particle characterization measurements without the need for additional image processing time. One such measurement incorporated into the design is roughness defined as "surface irregularity" and "jaggedness".

Examples of determining both a number and a mass distribution are given below. Although the examples relate to manual counting, the conditions also govern size analyses by automatic image analyzers.

3.2 Standards

Relevant national standards are available covering particle size analysis by microscopy. BS 3406 Part 4 [11] is the British Standard guide to optical microscopy. The American standard ASTM E20 was discontinued in 1994 [12]. ASTM 175-82 [13] is a standard defining terminology for microscope related applications. ASTM E766-98 [14] is a standard practice for calibrating the magnification of an SEM. NF X11-661 [15] is the French standard for optical microscopy. NF X11-696 [16] covers

general image analysis techniques. ISO/CD 13322 [17] is a draft international standard on image analysis methods.

3.3 Optical microscopy

Optical microscopy is most often used for the examination of particles from about 3 μm to 150 μm in size, although a lower limit of 0.8 μm is often quoted. Above 150 μm a simple magnifying glass is suitable.

The most severe limitation of optical transmission microscopy is its small depth of focus, which is about 10 μm at a magnification of 100 \times and about 5 μm at 1000 \times . This means that, for a sample having a wide range of sizes, only a few particles are in focus in any field of view. Further, in optical transmission microscopy, the edges of the particles are blurred due to diffraction effects. This is not a problem with particles larger than about 5 μm since they can be studied by reflected light, but only transmission microscopy, with which silhouettes are seen, can be used for smaller particles.

A two dimensional array of latex spheres is often used for measuring more or less uniformly sized lattices. Hartman [18-20] investigated the errors in this method which comprise focusing, image distortion, misreading of photomicrographs, distortions in the photographic material, anisotropy, other array defects, non-uniformity of particle size, coating of solutes on the lattices and contact deformation. Hartman introduced a new method, the center finding technique in which the latex spheres acts as lenses enabling the center-to-center distance to be determined with high accuracy (10 ± 0.4) μm for 10 μm particles. The National Physical Laboratory [21] introduced an NPL certified stage graticule [22] to test linearity over the complete image field.

3.3.1 Upper size limit for optical microscopy

The method is preferably limited to sub-200 mesh sieve size (75 μm) but larger particles may be counted and sized provided their fractional weight is less than 10% of the total weight of the powder. When the fractional oversize weight exceeds 10%, these particles should be removed and a sieve and microscope analyses merged. Alternatively such large particles can be sized using a simple magnifying glass.

3.3.2 Lower size limit for optical microscopy

The theoretical limit of resolution of an optical microscope is expressed by the fundamental formula:

$$d_L = \frac{f\lambda}{NA} \quad (3.1)$$

where d_L is the limit of resolution, i.e. particles in closer proximity than this appear as a single particle, λ is the wavelength of the illuminant, the numerical aperture of the objective $NA = \mu \sin \theta$ where μ is the refractive index of the immersion medium, θ is the angular aperture of the objective and f is a factor of about 0.6 to allow for the inefficiency of the system.

For $\lambda = 0.6 \mu\text{m}$ the resolving power is a maximum with $NA = 0.95$ (dry) and $NA = 1.40$ (wet) giving lower size limits, $d_{\min} = 0.38 \mu\text{m}$ and $0.26 \mu\text{m}$ respectively. The images of particles having a separation of less than these limits merge to form a single image.

The resolution of the human eye is around 0.3 mm, therefore the maximum effective magnification with white light is:

$$\frac{30 \text{ mm}}{28 \mu\text{m}} \approx 1000$$

Particles smaller than the limit of resolution appear as diffuse circles; image broadening occurs, even for particles larger than d_{\min} , and this results in oversizing. Some operators routinely size down to this level but the British Standard BS 3406 Part 4 [11] is probably correct in stipulating a minimum size of $0.8 \mu\text{m}$ and limited accuracy from 0.8 to $2.3 \mu\text{m}$. Powders containing material smaller than this are usually imaged by transmission or scanning electron microscopy and the resulting negatives or prints examined.

Charmain [23] in an investigation into the accuracy of sizing by transmission optical microscopy, showed that for two-dimensional silhouettes greater than $1 \mu\text{m}$ in diameter, the estimated size under ideal conditions was about $0.13 \mu\text{m}$ too high; a $0.5 \mu\text{m}$ silhouettes gave a visual estimate of $0.68 \mu\text{m}$ and all silhouettes smaller than $0.2 \mu\text{m}$ appeared to have a diameter of $0.5 \mu\text{m}$ (Figure 3.1). The measurements were made with the circular discs immersed in oil. Due to less precise focusing with three-dimensional particles, real particles are subject to greater errors.

Rowe [24] showed that wide differences in particle sizing can occur between operators because of this effect.

3.4 Sample preparation

Great care has to be taken in slide or grid preparation since the measurement sample is so small that it is difficult to make it representative of the bulk. Many particulate systems contain agglomerates and aggregates and, if it is necessary that they retain their integrity, the dispersing procedure needs to be very gentle. Further, since it is usually impossible to measure every particle in the measurement sample it is necessary that it be dispersed uniformly. Small regions selected at random or according to some predetermined plan must therefore be representative of the whole. The analysis is suspect if the regions in one area of the measurement sample give a very different size distribution to those in another area.

The simplest procedure is to extract samples from an agitated suspension; for less robust materials a procedure detailed in reference [3] may be used in which an air jet circulates the suspension through a sampling tube that can be closed and withdrawn to provide samples for analysis. Slides may be of three main types: dry, temporary and permanent. For very easily dispersed material, the particles may be

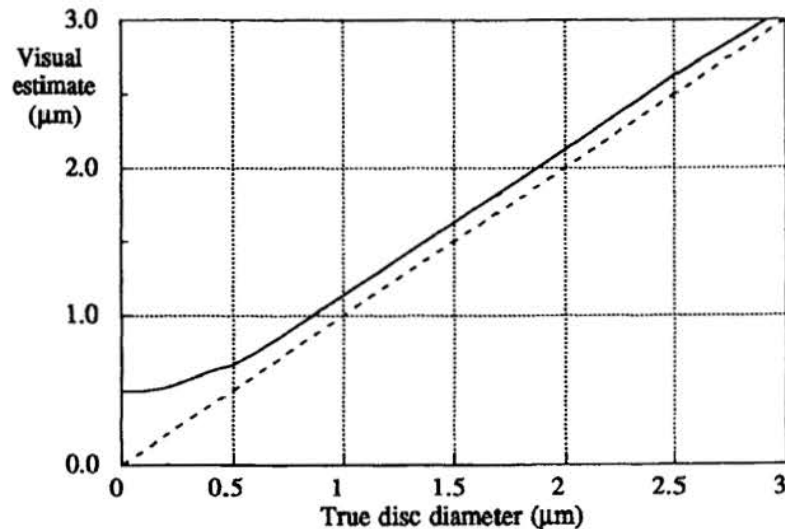


Fig. 3.1 Oversizing of small discs by optical microscopy [23]

shaken from a fine brush or the end of a spatula on to a slide. Humphries [25] describes a microsample splitter that assists the free flow of grains in order to provide the very small samples needed for microscopy: A diagram of the device is reproduced in a book by Hawkins [26]. Hawkins also describes a moving pavement version of the spinning riffler designed for preparation of representative samples of free flowing particles on microscope slides [27]. A novel method of mounting particles on regularly spaced adhesive circles has also been developed. This method of mounting results in an ordered array rather than the random chaos of usual methods and greatly facilitates particle analysis [28,29].

Some acceptable procedures for easily dispersed powders are described by Green [30] and Dunn [31]. For a temporary slide the powder can be incorporated into a viscous liquid, such as glycerin or oil, in which it is known to disperse completely. Some operators work the powder into the liquid with a flexible spatula; others roll it in with a glass rod. Either of these procedures can cause particle fracture and a preferable alternative is to use a small camelhair brush. A drop of this liquid can then be transferred to a microscope slide and a cover slip gently lowered over it. Rapid pressing of the cover slip must be avoided as it causes preferential transfer of the larger particles to the edge of the cover slip. It is undesirable for liquid to spread outside the limits of the cover slip; improved spreading is best effected with highly viscous liquids by pre-warming the microscope slide. Sealing the cover slip with amyl acetate (nail varnish is a good substitute) makes the slide semi-permanent. If low viscosity liquids are used it is necessary to have a well, or depression, on the slide to contain the dispersion.

The method of Orr and Dallevalle [32] for the production of permanent slides is to place a small representative sample of the powder to be analyzed in a 10 ml beaker, add 2 to 3 ml of a solution containing about 2% colloidon in butyl acetate, stir vigorously and place a drop of suspension on the still surface of distilled water in a large beaker. Prior to adding the suspension the surface is cleaned by allowing a drop of butyl acetate to fall on it. As the resulting film expands, it sweeps any particles on the surface to the walls of the beaker. As the drop of suspension spreads, the volatile liquid evaporates and the resulting film may be picked up on a clean microscope slide and completely dried. A dispersing agent may be added to prevent flocculation.

Permanent slides may also be produced by using the alternative combinations of Canada balsam or polystyrene in xylol, dammar in turpentine, gum arabic in glycerin, styrex in xylene, rubber in xylene and gelatin in water [33]. With a 1% solution this may be formed by dropping

it on to the cleaned surface of distilled water; with a 0.5% solution it may be cast directly on to a microscope slide; spreading is accelerated if the slide is first washed in a detergent.

Dullien and Mehta [34] use Cargill's series H compound, having a refractive index of 2.0, as a mounting medium for salt particles. This gives a transparent yellow background for the particles and, since it has a higher refractive index than salt, the particles appear as dark spots. A range of systems is necessary in order to select one where the difference in refractive index gives an easily detectable image.

Millipore recommend filtering a dilute suspension through a 0.2 μm PTFE membrane filter that is then placed on a dry microscope slide. The slide is then inverted over a watch glass half filled with acetone, the vapors of which render the filter transparent after two to three minutes.

Harwood [35] describes two methods for dispersing difficult powders. One involves the use of electrical charges to repel the particles then fixing the aqueous solution with a gelatin-coated slide to overcome Brownian motion. The other, for magnetic materials, involves heating the sample to a temperature above the Curie point then dispersing it and fixing it on a slide to cool.

Allen [36] mounted the powder directly into clear cement, dispersing it by using sweeping strokes of a needle and spreading the film on a microscope slide to dry. Lenz [37] embedded particles in solid medium and examined slices of the medium.

Particles may also be suspended in a filtered agar solution that is poured on to a microscope slide where it sets in seconds [38]. Variations in analyses between these procedures may occur due to particles settling on the slide with preferred orientations. Ellison showed that if particles were allowed to fall out of suspension on to a microscope slide they would do so with a preferred orientation. Also, if the dispersing is not complete, the presence of flocs will give the appearance of coarseness [39]. Pidgeon and Dodd [40], who were interested in measuring particle surface area using a microscope, developed methods for preparing slides of particles in random orientation. For sieve size particles, a thin film of Canada balsam was spread on the slide and heated until the liquid was sufficiently viscid, determined by scratching with fine wire until there was no tendency for the troughs to fill in. Particles sprinkled on the slide at this stage were held in random orientation. After a suitable hardening time, a cover glass coated with glycerol or warm glycerol jelly, was placed carefully on the slide. Sub-sieve powders were dispersed in a small amount of melted glycerol jelly. When the mixture started to gel a small amount was spread on a dry slide. After the mount had set, it was protected by a cover slip coated with

glycerol jelly. With this technique, it is necessary to refocus for each particle since they do not lie in the same plane. Several of these techniques were examined by Rosinski *et. al.* [41] in order to find out which gave the best reproducibility.

The sizing of fibrous particles by microscopy presents serious problems including overlapping. In order to minimize this it is necessary to work with only a few particles in the field of view at any one time. Timbrell [42,43] showed that certain fibers showed preferred orientations in a magnetic field, e.g. carbon and amphibole asbestos. He dispersed the fibers in a 0.5% solution of colloidon in amyl acetate and applied a drop to a microscope slide, keeping the slide in a magnetic field until the film had dried. For SEM examination an aqueous film may be drained through a membrane filter held in a magnetic field. In order to reduce overlapping to an acceptable level it is necessary to use a far more dilute suspension than for more compact particles.

Various means of particle identification are possible with optical microscopy. These include dispersion staining for identification of asbestos particles [44] and the use of various mounting media [45]. Proctor *et. al.* [46,47] dispersed particles in a solidifying medium of Perspex monomer and hardener. This was poured into a plastic mold that was slowly rotated to ensure good mixing. Microscope analyses were carried out on thick sections; a lower size limit of 5 μm was due to contamination.

Zeiss [48] describes a method for measuring sections of milled ferrite powder. The powder was mixed in 40:60 volume ratios with epoxy resin using a homogenizing head rotating at 25,000 rpm. The mixture was then poured into a 0.5 in diameter mold and cured at 60°C and 1000 psi to eliminate air bubbles. The casting was then polished in a vibratory polisher using 0.3 and 0.5 μm alumina in water. A photomicrograph of the polished section was used for subsequent analysis.

Automatic and quantitative microscopes tend to give erroneous results for transparent particles. To overcome this problem Amor and Block [49] a silver staining technique to make the particles opaque. The particles are dry-mounted on to a thin film of tacky colloidon on a microscope slide. Silver is then deposited from solution using the silver mirror reaction. Preliminary sensitizing the crystalline surface ensures that much more silver is deposited on the particles than on the colloidon. A method of staining particles in aqueous solution prior to deposition on a membrane filter for analysis is also given.

Hamilton and Phelps [50] adapted the metal shadowing technique for the preparation of transparent profiles of dust particles. The process consisted of evaporating *in vacuo* a thin metal film in a direction normal to

a slide containing particles. The particles are then removed by a jet of air or water, leaving sharp transparent profiles.

3.5 Measurement of plane sections through packed beds

When the size distribution of particles embedded in a continuous solid phase is required, the general approach is to deduce the distribution from the size of particle cross-section in a plane cut through the particle bed. The problem has occupied the attention of workers in diverse fields of science, who have tended to work in isolation and this has led to much duplication of effort. The historical development of this technique has been reviewed by Eckhoff and Enstad [51] and the relevant theory of Scheil by Dullien *et. al.* [52]. A theoretical analysis [53] has been criticized on several grounds [54].

Dullien *et. al.* [55-57] examined salt particles embedded in a matrix of Wood's metal using the principles of quantitative stereology. They then leached out the salt particles and examined the matrix using mercury porosimetry. Poor agreement was obtained and this they attribute to the mercury porosimetry being controlled by neck diameter. Nicholson [58] considered the circular intersections of a Poisson distribution of spherical particles to estimate the particle size distribution. Saltzman *et. al.* [59] generated a computer based imaging system for slices through a packed bed and found good experimental agreement.

3.6 Particle size

The images seen in a microscope are projected areas whose dimensions depend on the particles' orientation on the slide. Particles in stable orientation tend to present their maximum area to the microscopist, that is the smaller dimensions of the particles are neglected, hence the sizes measured by microscopy tend to be greater than those measured by other methods. Any one particle has an infinite number of linear dimensions hence, if a chord length is measured at random, the length will depend upon the particle orientation on the slide. These orientation dependent measurements are known as statistical diameters, acceptable only when determined in such numbers as to typify a distribution. They are measured parallel to some fixed direction and are acceptable only when orientation is random; i.e. the distribution of diameters measured parallel to some other direction must give the same size distribution. They are representative of the two largest particle dimensions, since the smallest is perpendicular to the viewing plane if the particles are in stable orientation.

Acceptable statistical diameters are:

- *Martin's diameter* (d_M) is the length of the line which bisects the area of the particle's projected area. The line may be in any direction, which must be maintained constant throughout the analysis [60,61].
- *Feret's diameter* (d_F) is the distance between two tangents on opposite sides of the particle parallel to some fixed direction [62].
- *Longest dimension*. A measured diameter equal to the maximum value of Feret's diameter.
- *Perimeter diameter* (d_c) is the diameter of a circle having the same circumference as the particle.
- *Projected area diameter* (d_a) takes into account both dimensions of the particle in the measurement plane, being the diameter of a circle having the same projected area as the particle. It is necessary to differentiate between this diameter and the projected area diameter for a particle in random orientation (d_p) since, in this case, the third and smallest dimension of the particle is also included.

The easiest diameter to measure is the Feret diameter but this is significantly larger than the other two diameters for most powders. It is probably best to reserve this diameter for comparison purposes and for rounded particles. Of the other two diameters, the projected area diameter is preferred since two dimensions are included in one measurement and the projected area is easier to estimate using globe and circle graticules than the length of the chord that bisects the image.

It has been shown [63,64] that the relationship between specific surface and Martin's diameter is:

$$S_v = \frac{4}{d_M} \quad (3.2)$$

Since the surface-volume diameter is inversely proportional to S_v , the constant of proportionality being a minimum of six for spherical particles, Martin's diameter is systematically different to the surface-volume diameter. Experiments confirm that, on the whole, $d_M < d_a < d_F$. The ratios of these three diameters remains fairly constant for a given material and may be expressed as a shape function. For example $d_F/d_M = 1.2$ for Portland cement and 1.3 for ground glass [65].

Heywood measured crushed sandstone which had passed through a 11/8 in. square aperture sieve and been retained on a 1 in. square aperture

sieve. He determined the projected area with a planimeter and calculated the mean projected diameter; he next estimated the diameter using both the opaque and transparent circles on a globe and circle graticule and also determined Feret and Martin diameters. His conclusion, based on an examination of 142 particles, was that the Feret diameter was greatly different to the other diameters for elongated particles, but that the Martin and projected area diameters are sufficiently in agreement for all practical purposes. This was disputed by Walton [66] who showed that the Feret diameter, averaged over all particle orientations, was equal to the other diameters. Herdan [67] examined Heywood's data more rigorously and found that:

- (a) The Feret diameter was significantly different from the other four diameters.
- (b) The Martin diameter showed significant difference from that obtained using the globe and circle graticule if the planimeter data were accepted as standard.

He concluded that there was no definite advantage to be gained by laboriously measuring profiles. As one might expect, the projected area diameters gave the best estimate of the true cross-sectional areas of the particles. This does not rule out the use of the other diameters if they are conveniently measured, since the cross sectional-area diameter of a particle is not necessarily its optimum dimension.

3.7 Calibration

It is necessary to use a calibrated eyepiece scale when carrying out a microscope analysis. The simplest form consists of a glass disc that is fitted on to the field stop of the ocular. Engraved upon the disc is a scale that is calibrated against a stage micrometer placed in the object plane; typically this is a microscope slide on which is engraved a linear scale. The image of the scale is brought into coincidence with the ocular scale by focusing. With a single tube microscope the magnification can be varied somewhat by racking the tube in or out. The stage graticule is then replaced by the microscope slide containing the sample. The microscope slide is made to traverse the eyepiece scale and particles are sized as they cross the reference line. Linear eyepiece graticules labeled 0 to 100 may be used to scan the sample so that the linear dimensions yields a size distribution as a function of the Martin or Feret diameter. Special graticules are also available containing globes (opaque images) and circles

(transparent images). The former are designed for the sizing of opaque images and the latter for transparent images.

3.7.1 Linear eyepiece graticules

These are linear scales, typically 10 mm, divided into 100 divisions of 100 μm , or 2 mm divided into 100 divisions of 20 μm each. They are placed in the focus of the microscope eyepiece so that they are coincident with the image of the microscope slide on the microscope stage. Calibration is effected using a stage graticule, 10 mm (100 \times 100 μm), 1 mm (100 \times 10 μm) or 100 μm (50 \times 2 μm), which is placed in the object plane.

Köhler illumination should be used [11] to give uniform illumination of the viewing plane. Using an oil immersion objective, it is possible to resolve down to about 1 μm , although a 15% oversizing is to be expected at this level due to diffraction effects.

Ocular graticules having a linear scale are satisfactory for the measurement of linear dimensions of particles. Particle sizes obtained with a linear eyepiece graticule are best classified arithmetically hence it is most suited to particles having a narrow size range.

3.7.2 Globe and circle graticules

Linear eyepiece graticules have been criticized on the grounds that the dimensions measured are greater than those determined by other methods. To overcome this objection, grids inscribed with opaque and transparent circles have been developed. For best results, opaque images are measured using the (opaque) globes while transparent images are best measured using the (transparent) circles. This permits direct comparisons between the projected areas of the particles and the areas of the circles. According to Cauchy the projected area is a quarter of the surface area for a random dispersion of convex particles [68] hence this measurement is fundamental to the properties of the powder.

The earliest of these graticules by Patterson and Cawood has 10 globes and circles ranging in diameter from 0.6 to 2.5 μm when used with a +2 mm 100 \times objective-eyepiece combination and is suitable for thermal precipitator work [69].

Fairs [70] designed graticules covering a size range of 128:1 using reference circles with a root two progression in diameter except for the smaller sizes. He considered this system to be superior to the Patterson-

Cawood where the series is much closer. He also described a graticule, having nine circles in a $\sqrt{2}$ progression of sizes, for use with the projection microscope [71]. This was incorporated in a projection screen instead of being in the eyepiece and was adopted by the British Standards Organization [11].

Watson [72] developed a graticule designed specifically to measure particles in the 0.5 to 5 μm (respirable dust) size range.

May's graticule, [73] covers 0.25 to 32 μm in a root two progression of sizes (the lower limit is highly suspect).

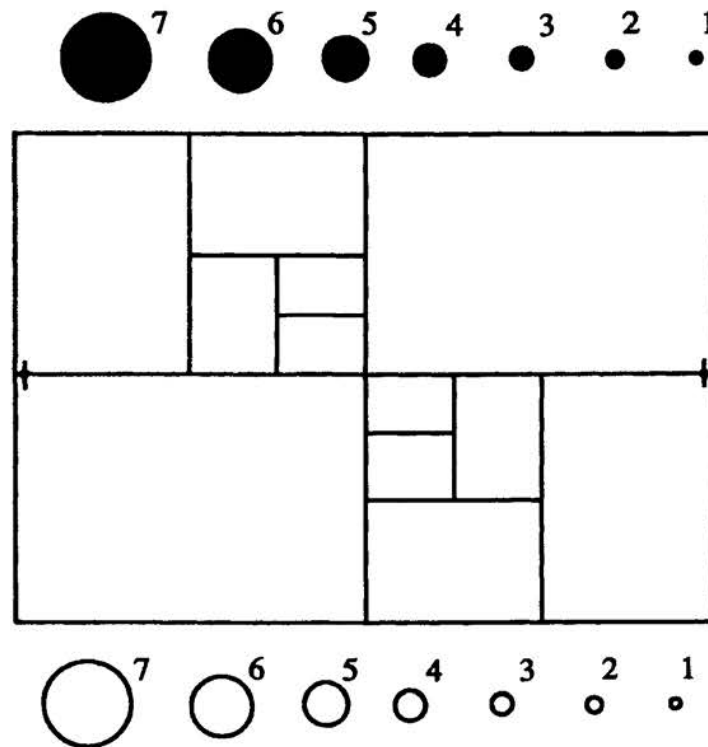


Fig. 3.2 The British Standard Graticule (Graticules Ltd) [11]. Diagram from BS 3406 (1963), Confirmed April 1993: *Methods for the Determination of the Particle Size of Powders: Part 4, Optical Microscope Method*. (Reproduced by permission from British Standards Institution, 2 Park Street, London W1, from whom copies of the complete standard may be obtained.)

[74] designed a graticule in which the diameters of eleven circles are arranged in a constant ratio of 1.2589 ($\log_{10} 1.2589 = 0.1$). He claimed that the choice of this ratio and the novel system of marking the circles facilitated the rapid calculation of size parameters from measured data.

The British Standard graticule is an improvement on Fair's graticule with seven globes and circles in a root two progression of sizes (Figure 3.2). With a +2 mm objective and a 20 \times eyepiece combination the minimum measurable size is about 1 μm . Circle 7 has a diameter eight times greater than circle 1; the grid has dimensions of 64 by 45.3 units with fiduciary marks at 60.4 units (circle 1 has diameter 1 unit). The graticule is divided into halves, quarters, eighths and sixteenths. Detailed setting up procedures are given in BS 3406 but, as an example, if the distance between the fiduciary marks is 566 μm the diameter of circle 7 is equal to 75 μm .

Particle thickness may be measured by a stereophotogrammetric method developed by Aschenbrenner [75, see also 32 p 19].

Hamilton and Holdsworth [76] compared the Watson graticule with a line graticule and with the Patterson-Cawood graticule. As the sizing of particles by visual comparison with reference circles some distance away from the particles may be subject to appreciable operator errors the line graticule was included in order to determine whether more consistent results were obtained by this method. With this type of graticule, particles are sized as they pass the reference lines and the diameter so measured is the Feret diameter. They found systematic differences in the mean counts of operators for the size range of 1 to 5 μm , but no evidence that this was affected by the type of graticule used. It was also found that the Feret diameter over-estimated the size of coal dust. Their conclusions were that all three graticules gave equally accurate and consistent results but the operators preferred the Watson and line graticules on the grounds that they were less trying to use.

3.8 Training of operators

Although the use of linear diameters such as Martin's or Feret's give the most reproducible analyses the projected area diameter is more representative hence the globe and circle graticule is the most popular. When comparing an irregular profile with a circle, untrained operators have a tendency to oversize the profile. A method of correcting this is to compare the analysis of a trained operator with that of a trainee. When the trainee recognizes the bias he readily corrects it. Heywood [77] produced a set of hand-held test cards pre-calibrated by counting squares. The trainee

is required to compare each of the profiles with reference circles and assign it to a size group. Watson and Mulford [78] extended the technique by inscribing a number next to each profile and reducing them photographically so that they could be examined under a reversed telescope, giving more realistic conditions. In a series of tests with nine operators, four were over estimating and five were under estimating, seven of the nine being badly biased. The nine operators were trained microscopists who were aware of the natural tendency to oversize and mentally corrected. The nine observers were consistent with their bias but reduced it only slightly on a second test.

Fairs [79] used a projection microscope for training purposes. This technique can also be used for size analysis [80] but is not recommended for particles smaller than 2 μm . Hamilton *et. al.* [81 *cit.*82] demonstrated the need to train operators and showed that gross count differences on the same samples at different laboratories were much reduced after inter-laboratory checks.

Nathan *et. al.* [83] compared three commonly used microscopic measurement techniques and confirmed oversizing by untrained operators. They suggested that unskilled operators produced the best results with a line graticule and that experienced operators perform best with an image splitting device.

3.9 Experimental techniques

The microscope should be set up using Köhler illumination; monochromatic illumination produces a better image if small particles are to be measured.

The microscope needs a vernier stage capable of moving the slide in two directions at right angles. The limits of the uniformly dispersed field are determined using a low magnification objective. Since it is impracticable to examine every particle on the slide, a sample is selected. Either isolated fields areas or strips are selected from the whole of the viewing area in order to smooth out local concentration variations (Figure 3.3). For a number count at least five strips 5 to 20 mm long need to be examined, the length of the strips depending on the density of particles on the slide, the whole area being such that at least 625 particles are counted. For a weight count, the requirement is that the area contains at least 25 particles in the largest size category. If these are few in number it is advisable to use strip scanning for counting the coarsest size categories. For particles that are present in quantity, the use of an eyepiece graticule containing a field area, as opposed to a linear scale, is recommended. In

either case the total area scanned must be determined in order that particle density on the slide (counts per mm^2) may be calculated.

When counting isolated fields, particles overlapping two adjacent sides are not counted. With strip counting, particles overlapping one of the edges are ignored; i.e. in Figure 3.3, shaded particles are included in count, unshaded particles are excluded otherwise the measured distribution will be weighted to the coarse sizes.

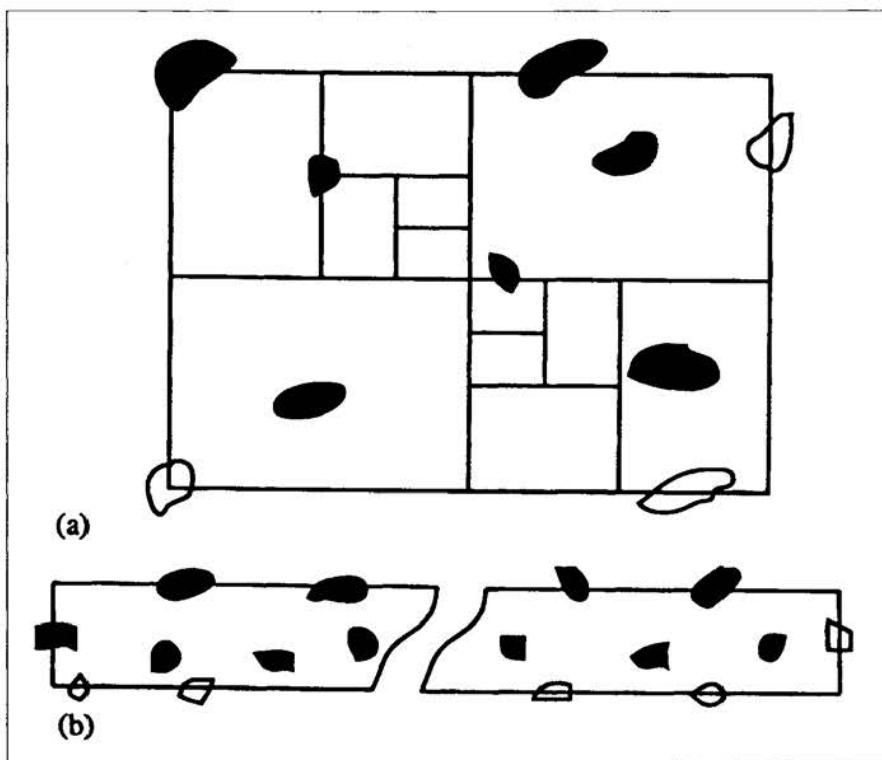


Fig. 3.3 Treatment of edge particles; (a) counting isolated fields, (b) counting strips

3.10 Determination of particle size distribution by number

Little difficulty is likely to be experienced in carrying out a number count since the same total area is used for all size classes and the minimum number of particles, namely 625, that it is necessary to count is specified in advance [equation (3.3)]. Let there be j classes of particles of interest. For

the r^{th} class ($r = 1, 2, \dots, j$) The number size distribution is calculated from the recorded values of the number m_r of particles of mean size d_r in j size classes found in sample area $A_r = n_r a_r$. For each class the number of particles per unit area is calculated m_r / A_r . Then p_r is calculated where:

$$p_r = \frac{(m_r / A_r)}{\sum_{r=1}^j m_r / A_r} \quad (3.3)$$

$100p_r$ is the number percentage in the r^{th} class.

The use of the British Standard graticule is illustrated in Table 3.1. The magnification is set so that the largest particle present in the field of view is smaller than circle 7. The magnification is then increased in order to accurately size the smaller particles. If there are particles present, which are smaller than the smallest circle on the graticule, a second increase in magnification may be necessary. Particles smaller than $2.3 \mu\text{m}$ are usually considered below the limit of resolution of the technique although this limit can be extended with loss of precision in the smaller size ranges. Sizes are often selected as an extension of sieve sizes i.e. 75, $75(\sqrt{2}/2)$, 37.5 and so on.

The class that contains the highest number concentration of particles (usually the smallest size class) is taken as the control size class.

The dispersion technique should give about 3 particles per field of view for these particles and at least 96 fields of view should be examined. At lower magnifications it is usual both to increase the area of the field of view and decrease the number of fields examined.

The expected standard error $s(p_r)$ of the percentage p_r by number in each size class, out of the total number in all size classes, is given by:

$$s(p_r) = \sqrt{\frac{p_r(100 - p_r)}{\sum m_r}} \quad (3.4)$$

where $\sum m_r$ is the total number of particles of all size classes. The standard error is a maximum when $p_r = 50$, hence $s(p_r)$ will always be less than 2% if $m_r \geq 625$. A statistical analysis has been carried out to determine the number of particles that need to be counted in order to construct a 95% confidence band over the whole sample. The measured size was the equivalent area diameter [84].

Table 3.1 Illustrative example of the calculation of a size distribution by number using the British Standard globe and circle graticule

| Circle number | Size limits (μm) | Total area examined (mm^2) | Number particles counted (m_r) | Cumulative number | Number frequency undersize | Expected standard error $s(p_r)$ |
|---------------|----------------------------------|--|---------------------------------------|-------------------|----------------------------|-------------------------------------|
| >7 | >75 | | 0 | 630 | 100.0 | |
| 7-6 | 75-53 | $32 \times 0.25 \times$ | 4 | 630 | 100.0 | 0.32 |
| 6-5 | 53-37 | $(75/8)^2 \times 0.064 \times$ | 8 | 626 | 99.4 | 0.45 |
| 5-4 | 37-27 | $0.0453 = 2.039$ | 6 | 618 | 98.1 | 0.40 |
| >7 | | | 19* | | | |
| 7-6 | 27-19 | | 18 | 612 | 97.1 | 0.66 |
| 6-5 | 19-13 | | 47 | 594 | 86.8 | 1.05 |
| 5-4 | 13-9.4 | $128 \times 0.50 \times$ | 39 | 547 | 86.8 | 0.96 |
| 4-3 | 9.4-6.6 | $(26.52/8)^2 \times 0.06$ | 154 | 508 | 80.6 | 1.71 |
| 3-2 | 6.6-3.3 | $\times 0.0453 = 2.039$ | 248 | 354 | 39.4 | 1.95 |
| <2 | <3.3 | | 106 | 106 | 16.8 | 1.49 |

- At high magnification, circle 7 is made equal to $26.52 \mu\text{m} = 75\sqrt{2}/4$ making field area $(26.52/8)^2 \times 0.064 \times 0.0453 = 0.0319 \text{ mm}^2$
- It is necessary to examine at least 100 fields and count over 625 particles and a quick check reveals that this can be done using half this area.
- At low magnification, circle 7 is made equal to $75 \mu\text{m}$ making field area $(75/8)^2 \times 0.064 \times 0.0453 = 2.039 \text{ mm}^2$ and, in order to examine at least 25 fields of total area 2.039 mm^2 , it is necessary to examine 32 fields using a quarter of the graticule area.
- This is an oversize check that should roughly agree with the count at low magnification.

3.11 Conditions governing a weight size determination

The percentage by weight in each class is:

$$q_r = \frac{(m_r d_r^3 / n_r a_r)}{\sum_{r=1}^j m_r d_r^3 / n_r a_r} \quad (3.5)$$

Direct conversion of a number count to a mass count leads to unacceptable errors. The omission of a single particle, in the largest size class (of

average size 63 μm in the previous example) is equivalent to the omission of over 10,000 particles in the smallest class (of average size 2.9 μm) i.e. the mass of a 63 μm particle is more than 10,000 times greater than the mass of a 2.9 μm particle. The expected standard error $s(q_r)$ of the percentage q_r in each size class, out of the total weight in all size classes, is given by:

$$s(q_r) = \frac{q_r}{\sqrt{m_r}} \sqrt{1 - \frac{q_r}{50}} \quad (3.6)$$

q_r is usually a maximum for the coarsest size range. Assuming this contains 10% by weight of the material and that a standard error of 2% is satisfactory, then $m_r = 20$ particles. This weight percentage should be calculated for each size class to confirm that in no case does it exceed 2%. For a weight distribution, the number of particles to be counted is governed by the number in the control size class. The number to be counted to achieve a given accuracy is:

$$s(M_g) = \frac{M_g}{\sqrt{m_r}} \quad (3.7)$$

$s(M_g)$ is the standard deviation expressed as a percentage of the total by weight;

M_g is the percentage by weight in the given size range;

m_r is the number of particles counted in the size range .

If it is estimated that 10% by weight of particles lie in the top size range and an accuracy $s(M_g)$ of 2% is required then it is necessary to count 20 particles in the top size range. In order to cater for errors in the estimate it is suggested that 25 particles be counted. It is The number density (N_r) is then calculated (particles mm^{-2}). The total count is maintained at about 700 by reducing the area examined for the smaller sizes. Briefly, the sample area required for particles of size d_r is:

$$A_r = \left(\frac{d_r}{d_0} \right)^6 \left(\frac{N_r}{N_0} \right) A_0 \quad (3.8)$$

where suffix '0' denotes the control class (the class containing the most particles by weight), which is usually the top size class.

A more comprehensive mathematical procedure to determine the number of particles to be counted in order to minimize errors has been proposed by Masuda and Inoya [85]. This procedure mandates a much higher count than the British Standard procedure presented here [86].

3.11.1 Illustrative example of the calculation of a size distribution by weight

This example is based on using the British Standard procedure [11]. At minimum magnification (circle 7 = 75 μm) the number of scans required to give 150 particles in the three top size categories is determined (Table 3.2).

Number of scans $n_r = 5$
 Length of scan = 10 mm
 Width of scan = $(64/8) \times 72 \mu\text{m} = 0.60 \text{ mm}$
 Area scanned $A_r = n_r a_r = 5 \times 10 \times 0.60 = 30 \text{ mm}^2$
 Number of particles recorded = m_r

Table 3.2 Preliminary examination of 5 scans, area 30 mm²

| Class | Size limits (μm) | Number of particles (m_r) | Number density $N_r = m_r / n_r a_r$ |
|-------|------------------|-------------------------------|--------------------------------------|
| 1 | 106-75 | 9 | 0.300 |
| 2 | 75-53 | 47 | 1.567 |
| 3 | 53-37.5 | 103 | 3.433 |

Number of scans required in order to count 25 particles in the top size class
 $n_1 = (25/9) \times 5 \approx 14$.

For other classes:

$$n_r = \left(\frac{d_r}{d_0}\right)^6 \left(\frac{N_r}{N_0}\right) n_1$$

class 2: $n_2 = \left(\frac{1}{\sqrt{2}}\right)^6 \left(\frac{1.567}{0.300}\right) \times 14 \approx 10 \text{ scans}$

class 3: $n_3 = \left(\frac{1}{2}\right)^6 \left(\frac{3.433}{0.300}\right) \times 14 \approx 3 \text{ scans}$

Nine more scans are completed for the top (control, $n_1 = n_0$) class size, during five of which particles in the second size class are recorded. The modified N values are determined and the above calculations repeated to ensure that a sufficient area has been scanned. The process is then repeated at a higher magnification (Table 3.3). Calibration for class 4 is that 60.4 units = 283 μm making the diameter of circle 7 equal to: $(8/60.4) \times 283 = 37.5 \mu\text{m}$.

$$\text{Area of graticule} = \frac{64}{60.4} \times \frac{45.3}{60.4} \times 0.283^2 = 0.0636 \text{ mm}^2$$

In class 6, particle density is high hence half the graticule is examined. The requisite number of fields is examined and the calculations carried out to ensure a sufficient area has been covered.

The process is repeated at a higher magnification (Table 3.4). Circle 7 is made equal to 13.25 μm making the distance between the calibration marks 100 μm and the field area 0.00795 mm^2 . 75 more fields need to be examined for class 7 only.

Table 3.3 Preliminary examination of 25 fields of total area 1.59 mm^2

| Class | Size limits (μm) | Number counted (m_r) | $N_r = \frac{m_r}{n_r a_r}$ | Required area (mm^2) [equation (3.7)] (A_r) |
|-------|----------------------------------|--------------------------------|-----------------------------|--|
| 4 | 37.5 - 26.5 | 21 | 13.2 | 6.6 = 107 fields |
| 5 | 26.5 - 18.8 | 44 | 27.7 | 1.77 = 28 fields |
| 6 | 18.8 - 13.3 | 79 | 99.4 | 0.79 = 25 \times (0.5) fields |

Table 3.4 Preliminary examination of 25 \times (1/4) fields of total area 0.0497 mm^2

| Class | Size limits (μm) | Number counted (m_r) | $N_r = \frac{m_r}{n_r a_r}$ | Required area (mm^2) [equation (3.7)] (A_r) |
|-------|----------------------------------|--------------------------------|-----------------------------|--|
| 7 | 13.3 - 9.4 | 9 | 181 | 0.193 |
| 8 | 9.4 - 6.6 | 8 | 161 | 0.020 |
| 9 | 6.6 - 4.7 | 7 | 141 | < 0.020 |
| 10 | 4.7 - 3.3 | 6 | 121 | < 0.020 |
| 11 | 3.3 - 2.3 | 4 | 81 | < 0.020 |

The data are tabulated and the standard error of the control size class determined to ensure that it is less than 2%. An accuracy factor is calculated for each size class and provided it is always less than the value for the control size class the standard error for the other size classes will be better than this. The completed table is shown as Table 3.5. Although the technique appears onerous, a skilled microscopist can carry out a weight analysis in about an hour.

3.12 Semi-automatic aids to microscopy

Semi-automatic aids to counting and sizing have been developed to speed up analyses and reduce the tedium of wholly manual methods. The advantage of these aids over fully automatic systems was that human judgment was retained. The operator could select or reject particles, separate out agglomerates, and discriminate over the choice of fields of view. Many such aids were developed and these differed widely over the degree of sophistication, price, ease of use, mode and speed of operation; they have however been supplanted by quantitative image analyzers.

The Zeiss-Endter analyzer [87,88] allowed a direct comparison between the projected area of the particle and the area of a reference circle that consisted of a spot of light adjustable in size by an iris diaphragm. The instrument was designed to work with a photomicrograph that could be obtained from an electron microscope to extend the lower size down to around 0.01 μm . Exnor *et. al.* [89] applied the instrument to size and shape determination of lead powder. A modified instrument, that was rugged and simpler but not as versatile, was described by Becher [90].

Crowl [91] used a projector, a transparent screen and a large transparent graticule to facilitate sizing from electron micrographs. The size was recorded via an electrical contact as the appropriate circle was touched by an electrical contact.

The basic module for the Digiplan [92] was an electronic planimeter with a built-in microprocessor. The image structure under analysis was traced out and stored in different count channels. Measured parameters were area and lengths that could be extended to other functions such as maximum diameter, form factor, centroid and so on.

The Chatfield comparator [93] was devised for the size classification of sub-10 μm particles from 35 mm film records and was based on the projection of a photograph on to a translucent screen which was back illuminated by a variable size light spot. When a match was made the operator used a foot switch to record the size.

Table 3.2. Illustrative example of a size distribution by weight using a British Standard Graticule

| Class number | Circle number | Size of class limits (mm) | Area of sample field (mm ²) (a) | Number of sample fields (n) | Total sample area (mm ²) (na) | Number counted in class (m) | Number conc. in class per (mm ²) (N = m/na) | Weight (d ³) | Relative weight in class (Nd ³) | Weight % in Class $q = \frac{100Nd^3}{\sum Nd^3}$ | Accuracy factor for class $F = \frac{Nd^3}{\sqrt{m}}$ | Weight size (mm) | Size dist. ⁿ % inclusive |
|--------------|---------------|---------------------------|---|-----------------------------|---|-----------------------------|---|--------------------------|---|---|---|------------------|-------------------------------------|
| 1 | >7 | 106 - +75 | 14x10x.6 | - | 84 | 27 | 0.321 | 741000 | 241000 | 9.6 | 46400* | 106 | 100 |
| 2 | 7-6 | 75 - 53 | 7x10x.6 | - | 42 | 66 | 1.571 | 262000 | 412000 | 16.4 | 50700 | 75 | 90.4 |
| 3 | 6-5 | 53 - 37 | 5x10x.6 | - | 30 | 103 | 3.433 | 92700 | 318000 | 12.7 | 30900 | 53 | 74.0 |
| 4 | 7-6 | 37 - 27 | 0.0636 | 120 | 7.62 | 98 | 12.86 | 32800 | 422000 | 16.8 | 42600 | 37 | 61.3 |
| 5 | 6-5 | 27 - 19 | 0.0636 | 30 | 1.91 | 53 | 27.75 | 11600 | 334000 | 13.3 | 45800 | 27 | 44.5 |
| 6 | 5-4 | 19-13.3 | 0.5x.0636 | 25 | 0.795 | 79 | 99.4 | 4100 | 417000 | 16.2 | 45800 | 19 | 31.2 |
| 7 | 7-6 | 13.3-9.4 | 0.25 x 0.00795 | 100 | 0.0199 | 36 | 181 | 1450 | 262000 | 10.4 | 30900 | 13 | 15.0 |
| 8 | 6-5 | 9.4-6.6 | 0.25 x 0.00795 | 25 | 0.0050 | 8 | 161 | 512 | 82000 | 3.3 | 10300 | 9.4 | 4.6 |
| 9 | 5-4 | 6.6-4.7 | 0.25 x 0.00795 | 25 | 0.0050 | 7 | 141 | 181 | 25400 | 1.0 | 3400 | 6.6 | 1.3 |
| 10 | 4-3 | 4.7-3.3 | 0.25 x .0159 | 25 | 0.050 | 6 | 121 | 64 | 7700 | 0.3 | 1100 | 4.7 | 0.3 |
| 11 | 3-2 | 3.3-2.3 | 0.0159 | 25 | 0.050 | 4 | 80 | 23 | 1800 | 0 | 200 | 3.3 | 0 |
| | | | | | | 487 | | | 2512900 | 100.0 | | | |

$$s(q_0) = \frac{9.6}{\sqrt{27}} \sqrt{\frac{1.96}{50}} = 1.66\%$$

- * Control size class. Standard error of control size class
- This should be smaller than the control size class for $s(q_0) < s(q_c)$. However the calculated standard error for this class is still less than 2% so this value is acceptable. If the error was too great more particles would have to be counted in this class.

The Lark counter [94] was designed for measuring particles in a loose powder, recording the sizes by the use of a series of pinholes in a chart. By ruling lines on the chart corresponding to a scale of sizes, and counting the pinholes between them, the size distribution in terms of the Feret diameter could be determined at a rate of about a thousand particles per hour.

The Watson eyepiece [95-97] used an image shearing principle whereby two images of the particle were produced and separated by the use of rotating mirrors. The distance moved was recorded so that the particle (shear) size could be found. An improved optical and mechanical system was claimed for the Vickers image splitting eyepiece in which the mirrors were replaced by prisms [98]. Timbrell [99] modified a normal microscope optical system by the introduction of a small mirror to reflect the light from the objective into the eyepiece. The mirror was mounted on the diaphragm of a loudspeaker vibrating at 50 Hz and illuminated at the extremities of the vibration. Because of the persistence of vision two images were produced. The energizing current controlled the amplitude of the mirror so that this was therefore proportional to particle size. The system gave high precision down to 2 μm [100]. A particular feature of Timbrell's device was that the images could be made to rotate in any direction so that they could actually 'dance' around each other thus permitting measurement of maximum and minimum diameters. The images could also be made to vibrate at two different amplitudes so that the overlap varied by down to 2 μm so that particles could be classified into narrow size categories [82]. An application of this system to difficult particulates has been presented by Perry *et. al.* [101].

Powder blends used for the manufacture of pharmaceutical products often consist of many ingredients and homogeneity can only be determined by using a technique that can discriminate between the ingredients. Manual microscopy is usually the answer where individual particles are identified and placed into size classes by comparing their images with a British Standard eyepiece graticule [102]. Manual methods are slow and tedious and automated methods, such as image analysis, are not always preferable.

The Zeiss AxioHOME (Highly Optimized Microscope Environment) was developed by pathologists to count, measure and analyze cell structure in biological thin sections. The AxioHOME is a light microscope coupled to a personal computer that allows the microscopist to make measurements on particles whilst still observing the real image. It is highly suited to particle size analysis because the measurements can be exported directly to a spreadsheet [103].

3.13 Automatic aids to microscopy

The need to count and size large numbers of samples of airborne dust stimulated the development of automatic microscopes. These instruments may be classified as spot or slit scanners [104]. The spot scan methods [105-107] were based on the flying spot microscope of Roberts and Young [108]. In this the scan was produced by a moving spot of light from a cathode ray tube which was projected through a microscope on to a specimen. When a particle interrupted the beam a photocell was activated and the particle counted. Special memory devices prevented the same particle from being counted twice [109]. However, certain designs of instrument were considered suspect, and there was always the possibility of re-entrant particles being counted twice [110]. In some instruments direct scanning was abandoned in favor of scanning a photographic image [111]. This extended the range of the instrument down to about $0.08\ \mu\text{m}$ but added an extra operation [91]. The theory of slit scanning has been covered by Hawksley [112] and the procedure was implemented in a commercial instrument [113]. In operation an image of the sample slide is projected on to a slit using a conventional microscope. The slide is mechanically scanned and the signals produced as the particle images pass over the slit are recorded. The reproducibility and accuracy were very good for spherical opaque particles down to $2\ \mu\text{m}$ in size [114].

3.13.1 Beckman Coulter RapidVUE

The *RapidVUE* analyzer can characterize fibers, powders, crystals, polymers and other materials at rates of 1200 particles per second. In the *RapidVUE*, fibers tend to be aligned with the direction of flow, making possible good measurements of fiber length, width and aspect ratio. The analyzable size range is $20\ \mu\text{m}$ to $2500\ \mu\text{m}$.

3.13.2 Micromeritics OptiSizer PSDA™ 5400

The *OptiSizer™ PSDA System* delivers continuous, on-line particle size analysis for materials with particles $45\ \mu\text{m}$ or greater. It consists of a CCD camera (with an internal image processor), a vibratory feeder, light source, monitor, keyboard and mouse. The camera captures high-speed images of the particles as they pass from the feeder through a controlled light source. The images are digitized and processed by the internal CPU. The software converts collected data into particle counts, diameters, areas and volumes. Form factoring is also available based on particle shape. Results are

displayed in both tabular and graphical formats. Digital outputs enable on-line statistical process control based on minimum and maximum particle size means. If the material varies from the acceptable range, an alarm can be triggered or it can be configured to control the process equipment.

3.13.3 Oxford VisiSizer

VisiSizer is a direct imaging system that combines a pulsed laser to freeze subject motion, a digital camera to capture frames at high or low speed and a computer to display and analyze images. The *VisiSizer* range offers image exposures from 30 nanoseconds to 1 microsecond, image capture from 30 to 10,000 frames per second, with digital cameras of varying resolution. Software uses Particle Droplet (including bubbles) Image Analysis to rapidly analyze particles and droplets. Images can be analyzed directly or fed to a hard disc. Software analyzes 3 frames per second and the laser is pulsed twice per frame to give velocity as well as size. Slightly out of focus images can be accurately measured by examining edge gradient.

3.13.4 Retsch Camsizer

The *Camsizer* measuring system is based on digital image processing. The dry powder flows between a light source and camera and the particles are detected as projected areas, digitized and processed. During the measurements two digital full-frame cameras perform the particle analysis: The basic camera detects the large particles and a zoom camera registers the small. The theoretical measurement limits are 15 μm to 90 mm with a practical range of 30 μm to 30 mm. Electronic processing of the images takes place internally in 10,000 size classes and saved in a 1000 size classes. Graphical representations of the results are available while the measurement process is still running. The computer calculates all standard particle distributions together with microscope shape factors such as Martin and Feret diameter, longest chord and so on.

3.13.5 Malvern Sysmex Flow Particle Image Analyzer FPIA-2100 automated particle shape and size analyzer

Particles are sampled from a dilute suspension and held in an agitated chamber to ensure it is kept in suspension. The particles are introduced into a sheath flow through a jet nozzle. The sheath flow transforms the suspension into a flat, narrow stream through hydrodynamic focusing. The

sheath flow ensures that the largest projected area of the particle is oriented towards the video camera and all the particles are in focus. The cell is illuminated with a stroboscope and images of the particle are captured at 30 Hz. The particle images are processed in real time by digitizing, edge highlighting, binarization, edge extraction, edge tracing and image storage. If there are 7 particles per image a total of 25,000 particles are captured and analyzed. Typically, comprehensive particle data are generated in less than 5 minutes. A computer calculates the area and perimeter of each of the captured particle images and then calculates the particle diameter and circularity. A high power field ($\times 20$) covers the particle size range $0.7\ \mu\text{m}$ to $40\ \mu\text{m}$ in 3 size classes and a low power field ($\times 5$) covers the size range $4\ \mu\text{m}$ to $160\ \mu\text{m}$ in 4 size classes.

Once the measurement is complete, particle size and distribution data are displayed in graphical and tabular form. A typical result report includes three plots; particle size distribution, circularity distribution, and a scattergram of particle size versus circularity. Individual particle images are captured and displayed and these can be classified by the operator into various categories. The instrument is covered by US patent No 5,721,433.

3.13.6 Sci-Tec PartAn - video Image Analyser

Particles are dropped between a video camera and a synchronized strobe light. When the strobe flashes, the camera takes an image of the particle which is digitized by a computer frame grabber. For samples with a wide size range two cameras can be used simultaneously, one with high magnification and one with low. Particles are measured for area, perimeter and minimum and maximum diameters. From these measurements shape factors, aspect ratios and volumes are calculated. Thousands of particles can be measured in each digital image and images can be acquired at 20 frames per second. Total analysis time is 3 to 5 minutes. Size and shape are displayed in particle size and sieve size bins. Shape and aspect ratios are displayed by size fraction. Totals and averages are also displayed. Size range covered is from $10\ \mu\text{m}$ to 6 inches.

3.14 Quantitative image analysis

Manual methods of obtaining data from images are slow and tedious and this can give rise to considerable error. The introduction of fully automated image analysis systems has virtually eliminated manual methods and also supplanted semi-automatic systems. All image analysis systems use scanning techniques for converting images into electrical signals that are

processed to yield data on the images. If the microscope is fitted with an automatic stepping stage and autofocus, it is possible to measure large numbers of fields of view, thus greatly improving the statistical accuracy. However, image analysis systems cannot discriminate artifacts as readily as human operators and are unable to adjust focus during measurements in the field of view, which can cause problems with particulate systems having a wide size range. With automatic image analysis, not only is it necessary for particles to be singly dispersed, they should also be clearly separated from each other so that the analyzer is not confused by touching particles [115].

3.14.1 Calibration of image analyzers

The procedure for calibration of image analyzers varies from machine to machine. It usually involves indicating on a screen the dimensions of an imaged artifact of known dimensions. This may be a grid, grating, micrometer or ruler and the dimensions are usually expressed as pixels per unit length. The calibration should be carried out both parallel to, and perpendicular to, the scan direction. Image analyzers may also suffer from localized distortion, which may be detected by comparing a square grid with an overlaid software generated pattern.

The National Physical Laboratory [21] introduced a certified graticule to test the linearity of a scanner over the whole field, the resolution obtained and the effect of gray level detection on the measured size distribution. It has four separate fields: A major field divided into smaller proportional fields, an array of equidistant monosize circles, a root-two by diameter array and a log-normal number/diameter distribution in an equi-centered array. The value of this, commercially available graticule has been illustrated by its use on a Quantimet 900 [22]. Polystyrene spheres (5, 7, 10 and 15 μm) have also been used for calibration and the results compared with SEM and Coulter data [116].

3.14.2 Experimental procedures

Automatic image analysis is a six step process (Figure 3.4); (1) image formation, (2) image scanning, (3) feature detection, (4) feature analysis by count, shape, size or other selected parameter, (5) data processing and analyzing; (6) data presentation.

Image formation is a crucial step in image analysis. Quantitative image analyzers consist of a high linearity television camera that can be interfaced with a microscope, macroviewer or videotape. An electron probe interface

can be used to accept image inputs from scanning electron microscopes, microprobes or acoustic microscopes [118-120]

The macroviewer is used to analyze large objects such as 8 in by 10 in photographs. Large objects and photographs can be illuminated with incident light; transparencies and slides by transmitted light. The electron probe stores whole images generated by the SEM and converts them into a proper form for analysis.

Signals from the image received by the camera are processed by a central processing unit that contains circuits for measuring areas of features, number counts and size distributions based on selected diameters. Parameters such as ratio of maximum to minimum diameters may also be determined. The area under examination is displayed on a screen and interaction is either via a teletype keyboard or menu driven. Using this unit, objects can be selected for examination, objects can be deleted and touching particles can be separated.

Image editing and classification features such as picture enhancement using gray level detection to enhance contrast are often available (Figure 3.5). Surface texture analysis, fractal dimension determination, shape regeneration using Fourier analysis, angularity and roundness measurement may also be carried out. The resulting distributions are presented graphically in a wide variety of modes and the data may be stored for further interrogation.

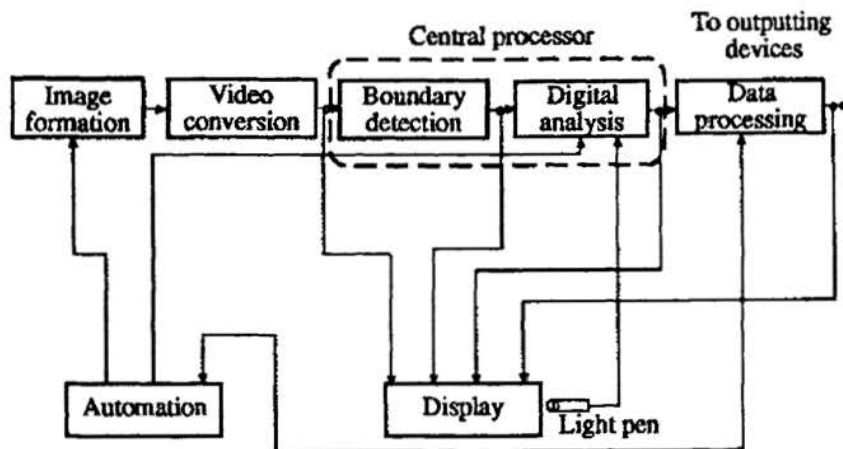


Fig 3.4 Block diagram of image analysis system, indicating the six major functions[117]

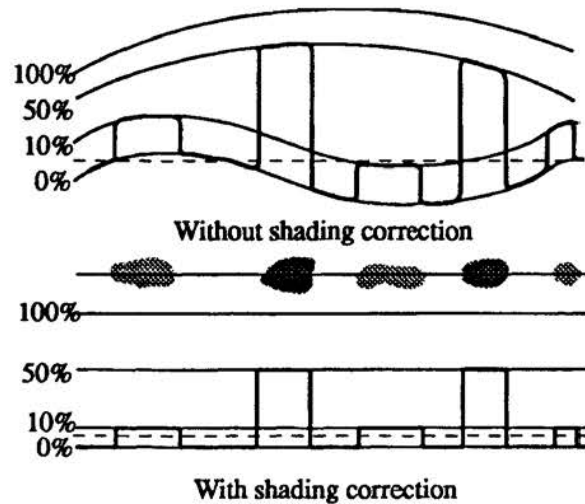


Fig. 3.5 Gray level shading correction the objective of the gray level detection function is to define in the images the boundaries of features that are to be counted and measured (Bausch & Lomb, Omnicon).

Images require a great deal of computer memory because an image is actually an array of numbers; i.e. intensity at every location $I = f(x,y)$. For a 512 by 512 digital image, over a quarter of a million numbers must be stored. Consequently, until recently, most image analysis was done on large computers or with dedicated image processing hardware. It is now possible to do a great deal of processing on a workstation computer.

Most digital image operations fall into one of two categories [121] namely image processing and image analysis. Image processing operations turn one image into another image; for example, edge finding or crispening. Operations that quantify some aspect of the image, such as area fraction or average particle size, are called image analysis. In general one would prefer to do little or no processing in order to save time and not alter the original image. However it is often necessary to do some processing to prepare an image for analysis [122]. An image can be digitized from a video camera attached to a light microscope or on a copy stand to digitize either the particles themselves or a photomicrograph. Images can also be digitized from one of the contrast-bearing signals from a microscope. Once digitized, the images can be stored for later analysis and processing or for archival purposes.

A digital image has a discrete number of pixels (picture elements), each of which contains an intensity value, usually scaled from 0-255. The

number of pixels determines the resolution with 512 by 512 being the most common.

Theoretically, image resolution is limited only by computer memory; however it is usually not possible to display more than 1024 by 1024 and PC class computers may not be able to display 512 by 512. For most practical purposes 512 by 512 is adequate but higher resolution is useful for analyzing large and small features at the same time.

Each pixel in the image is digitized to a limited number of gray levels depending on the hardware used. The human eye has a range of 1010 brightness levels that it can adapt to but it can only discriminate about 20 levels at a time. Older image systems provide 64 or fewer levels but newer ones commonly provide 256. Such a large number of gray levels is necessary for discriminating phases on the basis of their brightness but may not be necessary for particle characterization.

The computer compares several focal planes and the sharpest image selected. The software then corrects the brightness until it is approximately constant over the whole image. The image is then binarized: All pixels below a certain gray level become white and the rest become black or vice versa; with this procedure particles can be differentiated from background. The height of the binarization threshold has an influence on the number of black pixels and its selection is a multiple step procedure [123].

Some of the binary particles may contain bright spots. This happens especially with transparent particles in transmission microscopy. These spots have to be closed.

Although the human eye can only discriminate about 20 levels of intensity simultaneously, it can distinguish about 350,000 different shades of color. The significance of this is that pseudo color can be used in an image to convey details that would otherwise be lost in a gray scale image.

In general, the goal of image processing is improving the image, but the only thing certain is that the image is changed. No information can be extracted that was not present in the original image and artifacts can be introduced. One example of a need for image processing would be separating overlapping particles (Figure 3.6).

- *Resolution* is determined by the number of pixels (picture elements): The measured particle area is the number of elements multiplied by the elemental area; the particle perimeter is the number of edge element multiplied by the length of the sides.
- *Erosion* In order to separate touching images, the edge pixels are removed together with any touching pixels within the image.

- The residual pixels make up smaller non-touching images; the smaller image disappears completely.
 - *Dilation* In order to create new non-touching images a peripheral layer of pixels is applied.
- When a second layer of pixels is added, the original image is reformed with some loss of detail and the two touching images are separated.

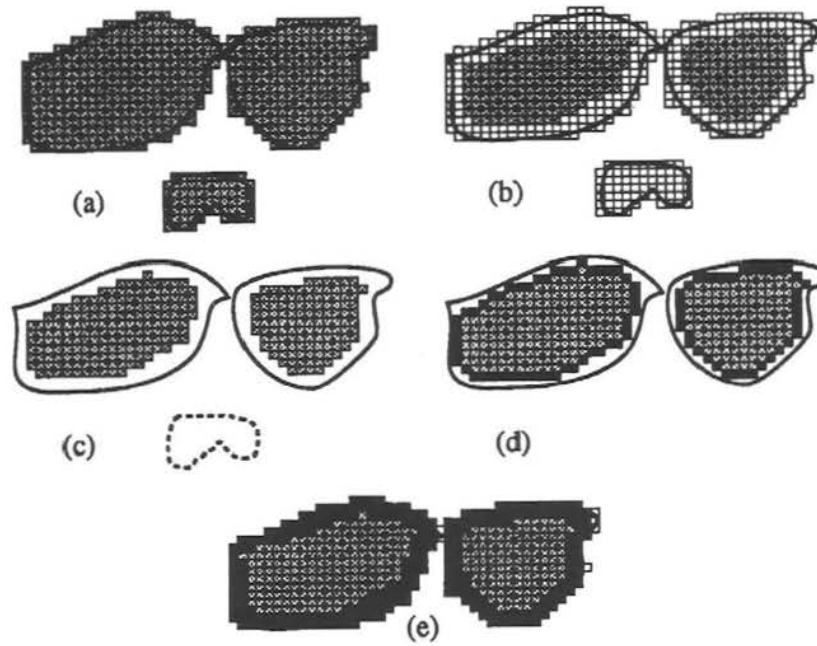


Fig. 3.6 Separating overlapping images using erosion and dilation.

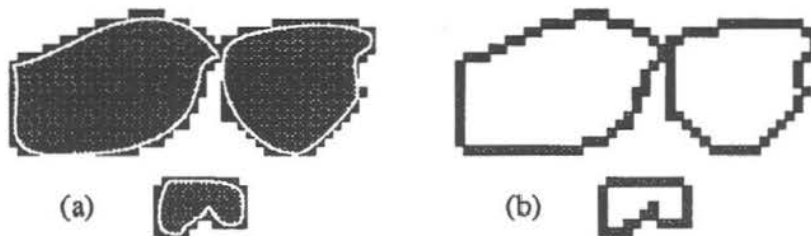


Fig. 3.7 (a) Area and (b) perimeter measurements by quantitative image microscopy[124].

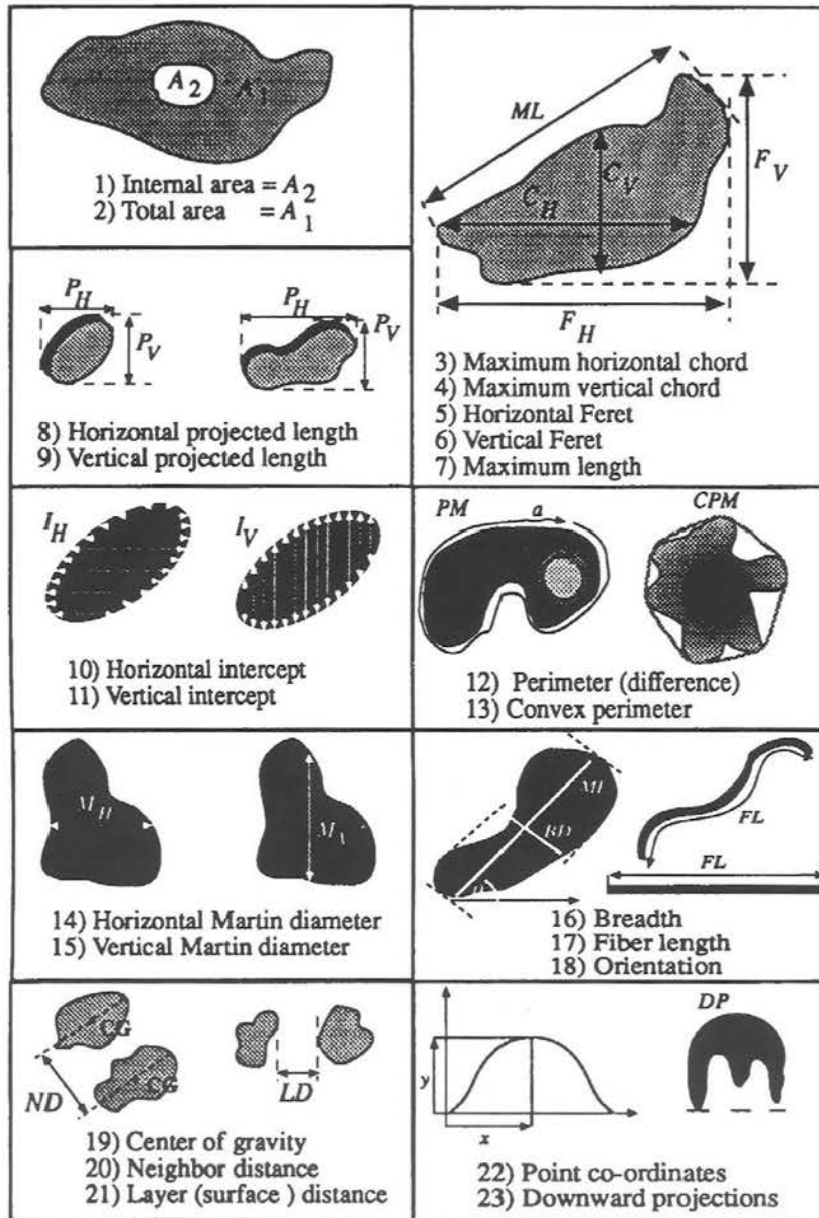


Fig. 3.8 Measured parameters by quantitative image microscopy.

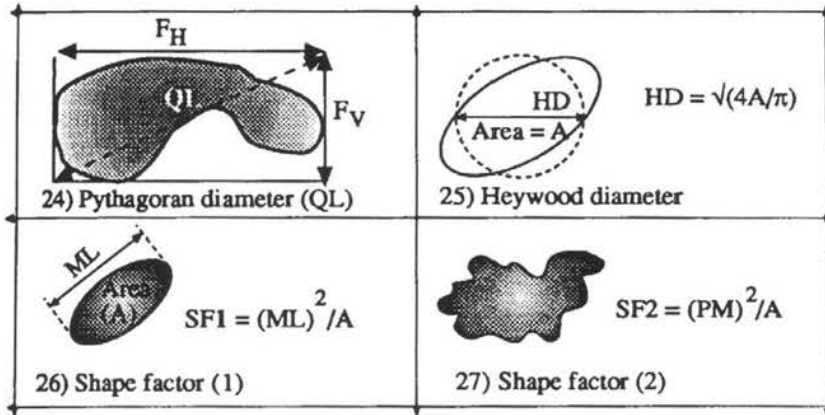


Fig. 3.8 (Cont.) Measured parameters by quantitative image microscopy.

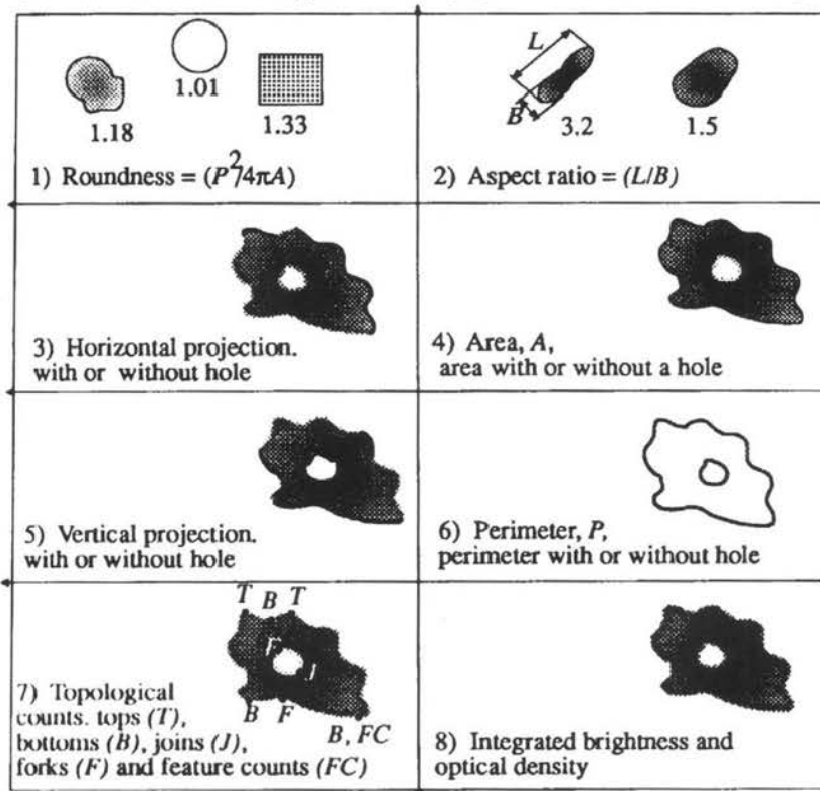


Fig. 3.9 Shape factors of image analysis systems.

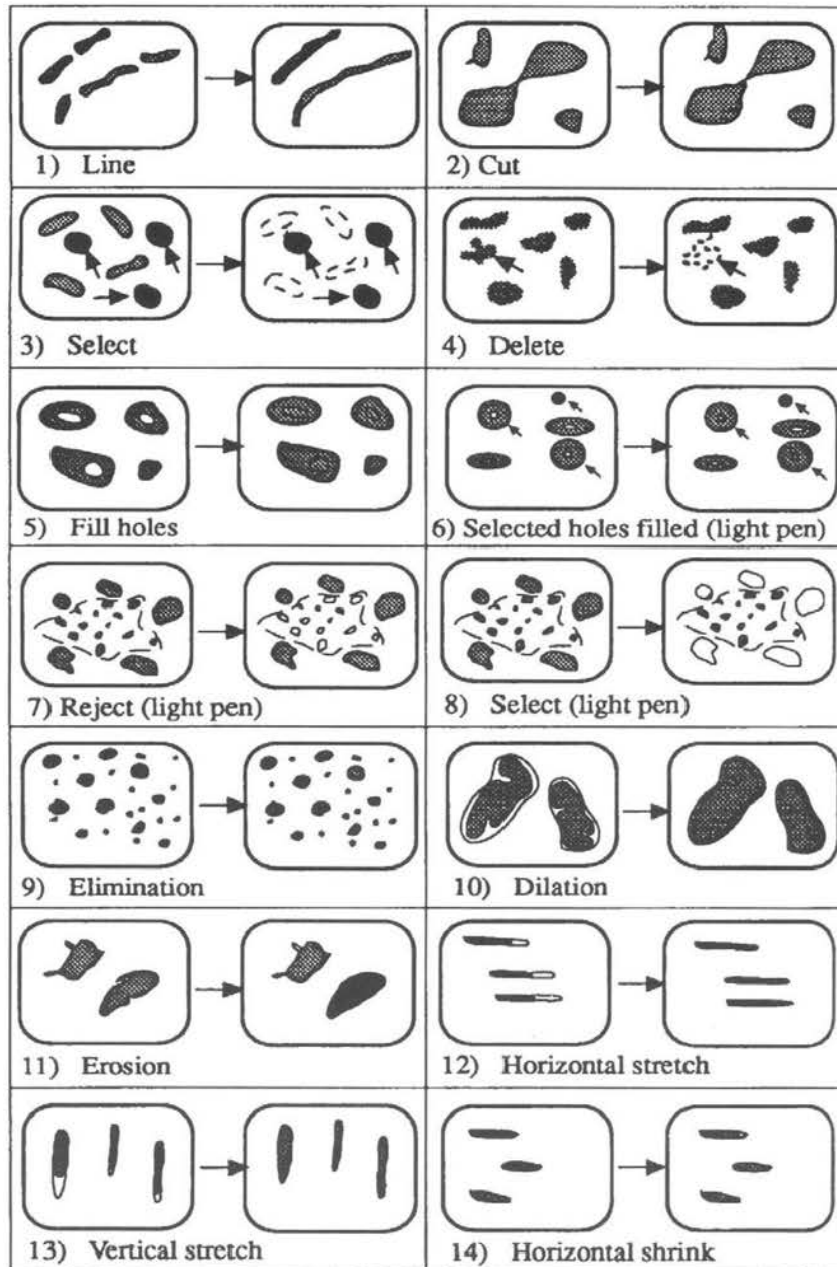


Fig. 3.10 Editing features of image analysis systems.

Erosion and *dilation* results in some loss of information. Simple operations such as erosion and dilation or complex operations such as artificial intelligence can accomplish this task. If these fail, the operator, using a light pen, can cut features apart. Gray level erosion and dilation has been studied to characterize the particle size of powders in bulk. The procedure was tested using mixtures of steel balls, from 0.3 to 1 mm, in diameter and ground pea kernels [125]. The results, using a Trydin image analysis system, agreed reasonable well with laser diffraction data.

Other forms of image processing operate on the entire gray scale image and transform the contrast. Some uses for these operations include background smoothing, crispening, edge detection, noise removal and the enhancement or suppression of periodic information.

The systems available today are both more sophisticated and simpler than before. The trend is towards more automation, greatly increased speed, more sensitivity and improved camera technology, particularly the use of CCDs.

Specifically, many systems are based around or incorporate parallel processing hardware so that image pixels can be processed simultaneously, providing faster throughput and allowing highly complex algorithms to be supported. Fibers can be aligned, touching particles can be separated, particles can be selected for measurement and deleted holes can be filled. A light pen is often provided so that features can be selected for acceptance or rejection. Particles can be dilated or eroded for image enhancement, and fibers may be stretched or shrunk to create a better image.

The application of quantitative image analysis to size (area) and perimeter determination is demonstrated in Figure 3.7. The image analyzer sees only two images since the larger images overlap. The larger image (Figure 3.7a) has an area of 552 square units made up of 325 LHS (left hand side) and 227 RHS (right hand side) and the smaller image has an area of 66 square units (assuming the area occupied by one pixel is one square unit). The pixels that overlap the edges of the image define the perimeters (Figure 3.7b). The larger particle(s) have a perimeter of 134 units LHS and 73 units RHS and the smaller particle has a perimeter of 36 units. Thus, as in fractal geometry, the smaller the pixel the greater the perimeter. The contour following algorithm depends upon the chosen connectivity of the pixels (i.e. the number of touching pixels within the image).

Some other parameters that can be measured by quantitative image microscopy are illustrated in Figure 3.8; shape factors are illustrated in

Figure 3.9 and editing features in Figure 3.10. Serra [126-128] developed the method of mathematical morphology in image analysis and the theory was extended by Matheron [129,130].

The basic operation involves erosion and dilation procedures to produce a modified image picture from the original. The major disadvantage of this procedure is the requirement for large memory space. This problem was resolved by use of a compressed data technique for binary image pictures [131].

Davidson *et. al.* [132] compare image analysis to other methods of particle size measurement. They used a Magiscan image analyzer with Genias™ particle sizing software. The images were generated with a Zeiss universal microscope equipped with Optovar and bright field optics and acquired using a Dage-TI camera model 70 with a green filter. Calibration was with a Bausch & Lomb ruled stage graticule. The gray levels were converted to binary and touching particles were separated manually. Various parameters were measured and data compared with data generated by sieving, using a Hiac PA 720 (operated with dry powder) and the Coulter Counter TA II.

It was deduced that the cut size for the sieves was controlled by the breadth of the particle (as expected) and the measured parameter by Hiac was also controlled by breadth rather than equivalent spherical diameter as one would expect. If multiple pictures of the particles, taken from different directions, are available then a three dimensional image can be reconstructed and the 3-D convex hull reconstructed [133].

Automated image analysis has also been used to characterize the degree of mixing in a drum mixer. Different colored glass beads were placed at the front and rear end of the mixer and were set in place after mixing using solidification techniques. The bed was then sliced and the slices scanned with a video camera to produce digital images. The mixture quality of elements within each slice was next determined using an image analyzer. This procedure enabled a spacial determination of mixture quality both along the axis and within bed depth [134].

For automatic image analysis of fibers it is necessary to generate an image with a limited number of overlapping fibers. A method of generating such a distribution with dry fibers by impacting the particles on an inclined plate and subsequent sedimentation on to a microscope slide has been described [135]. For wet sample preparation the suspension was first dispersed, then deposited on a membrane filter for examination by reflected light or transmitted light after first making the filter transparent by a chemical agent. An alternative method of preparation, by allowing the fibers to settle out of suspension on to a microscope slide, was also used.

Schäfer, [136] in a discussion on the accuracy of image analysis systems, states that the accuracy of area and equivalent diameter measurements is sufficient for most practical purposes. On the other hand he suggests improvements in the determination of perimeters and shape factors which he found to be unsatisfactory.

3.14.3 Commercial quantitative image analysis systems

American Innovation Videometric 150 readily measures and counts specific features in an image. The system incorporates threshold monitoring so that images within selected brightness levels are selected. Editing is provided with the use of an adjustable paintbrush with the mouse to include or exclude any parts of the image. In this way objects that appear separated may be connected or objects that wrongly appear as one may be separated. The erosion routine reduces every detected feature by one pixel at a time over the entire boundary. This process breaks bridges and opens pores. During dilation pixels are added one at a time to smooth surfaces and fill in bays.

Analytical Measuring Systems features *Quickstep*, a sophisticated control system for precise positioning of microscope stages and macrostages in *X*, *Y* and *Z* axes with the added facility for automatic focus. As a 'standalone' system it offers versatile semi-automatic and fully automatic control for scanning selected areas of a specimen. Alternatively it can be used in conjunction with a microcomputer to run application programs or as an integral part of an AMS image analysis system. *VIDS V* is an interactive image analyzer that provides a means of quantifying images not suitable for gray level analysis. An image, which can be viewed in color or monochrome, may be analyzed by tracing around, or along, features; or by placing dots across them using a digitizing pad and cursor. The standard software provides all the measurements and statistical tests. A low cost alternative to *VIDS V* is found in *Measuremouse*, which features a high resolution CCD camera to view the sample and display the image on its graphic monitor. Objects selected for measurement are inscribed using a mouse-driven cursor and their size and shape determined via an Amstrad personal computer. Comparison of measured parameters and the generation of size or shape distributions are carried out using spreadsheets such as *Super Calc* and the results provided via a high speed dot matrix printer. *Optomax V* is a fully automated image analysis system with a high spatial precision of 704 by 560 pixels. These systems are available in the USA from *Optomax Inc.*

Artek market a range of image analyzers. The *Artek Omnicon 3600* is an advanced, easy to use system with turnkey application software. A precision scanner converts optical images into video signals that are presented on a high resolution monitor screen. The required measurement is selected from more than 20 parameters. The measure key is pushed and the answer appears ready to be printed out, saved or exported to any of a wide range of data bases and spreadsheet programs

Automatix produces automated image analysis packages comprising data collection, spreadsheet analysis and charting to be used with the Macintosh computer. This has been used, in conjunction with ancillary equipment, to produce a computer digital analysis system [137] for around \$4,000 [138]. Later, a more sophisticated system, costing around \$20,000, was described for digital examination of film.

Boeckeler manufacture simple systems which require more operator input but are less expensive than more automated systems. The *VIA-20 Video Image Marker* can be used to mark details on a video image; the *VIA-50* includes a more varied array of positionable markers with an option for multiple overlay storage; the *VIA-100* can perform horizontal, vertical and point-to-point measurements, and the *VIA-150* combines the capabilities of the *VIA-50* and *VIA-100*. The *VIA-160A1* video area measurement system can be combined with a video microscopy system to give cell areas, chord lengths and number counts.

Buehler Omnimet II is a high resolution automatic image analysis system.

Compix C-Imaging 1280 System has an image input of 1024×1024 resolution and uses the latest hardware to achieve high speed processing and analysis. The 1280×1024 non-interlaced 19 in. color monitor provides viewing quality for user comfort. The system is complemented by *Simple*© imaging software to give user flexibility in an uncomplicated framework. The system can enhance, identify and count 1000 objects in less than 1 s, measure the data and perform summary statistics in less than 3 s, and provide histograms at the touch of a button. The *C-Imaging 640* system has a color or monochrome input with a resolution of 640 by 640. The system benefits from high speed processing and analysis hardware.

Data Translation market *Global Lab Image* that captures and digitizes images, then displays, processes and analyzes them. A complete set of algorithms is provided which work with any imaging device. The programs are used with Microsoft Windows™ for scientific word processing, statistics, spreadsheet analysis or data plotting.

Hamamatsu C-1000 is a computer compatible video camera that can be mounted on a microscope, macroviewer, optical bench or tripod. The

number of particles can be tabulated based on specified parameters. Information can be input and analyzed by the computer.

Hitech Olympus Cue-3 is a color image analysis system with a wide range of image enhancement and processing capabilities.

Joyce Loebel Magiscan is a total image analysis system which can be interfaced to a wide range of optical and electron microscopes. The general purpose menu and results programs provide flexible means of extracting particle size and shape information [139].

Leco offer several image analysis systems. The AMF-100 is dedicated to microhardness measurement and the 2005 is a top of the line, high performance system. The 2001 is a mid-range general purpose image analyzer. The 3001 operates using Microsoft Windows™. The system can interface with a broad range of peripherals and has the ability to archive images for later processing.

Leco IA32 is a versatile image analyzer suitable for users with varying levels of expertise. Although designed primarily for the metallographer its other applications include the measurement of porosity, grain size, area fractions, number count, particle size, fiber length and dendrite arm spacing.

Leica Quantimet 500 costs less than \$15,000 complete and can be used with any microscope. The single display combines menus and images through PC based Windows™ graphical user interface.

LeMont Oasy image analysis system acquires, enhances, measures and classifies images. The Omega system forms a high quality bridge between a PC and SEM.

Maztech Microvisions Spy grain grader is an image analysis benchtop instrument that uses linear CCD arrays to determine objective grade and non-grade factors in grains and seeds [140].

Millipore π MC System offers speed and precision in counting particles, determining size distributions and characterizing shapes.

Nachet 1500 is a processor specifically designed for image analysis. The image is acquired with a TV camera and directed to the Nachet 1500 for image processing and measurements. The results are sent to an Apple IIe type computer to drive the various peripheral devices associated with the topic being studied. The microcomputer is also used for setting up the instruction sequence for image processing and for running programs.

Nikon analytical microscopy workstation Microphot SA is adaptable for complex multi-imaging requirements run from a host computer.

Oncor Instrument Systems (formerly *American Innovision*) designs and manufactures its own hardware and software which incorporates multiple

true color analysis models, multiple thresholds and low light true color CCD cameras.

Optomax V is a simple to use automatic image analysis system employing dual microprocessors combined with high speed measurement circuitry. The system uses up to four high performance TV cameras to provide direct viewing of macroscopic or microscopic images. It counts and measures image features such as area, perimeter, Feret diameters, horizontal and vertical intercepts and so on.

Outokumpu Imagist is a medium priced unit which bridges the gap between the limited capability PC systems and the high cost, hardware based systems.

PharmaVision 830 (Malvern) measures dry powders in the size range 0.5 μm to 2000 μm . A range of optical configurations is available together with a range of presentation plates (microscope slides). A comprehensive list of size and shape parameters can be measured together with custom parameters.

Shakespeare Corporation's Juliet features single particle size and shape measurement together with fractal analysis as well as conventional classical measurements. It also measures size and shape distributions for sets of particles with image manipulation and data graphing capability.

Tracor Northern manufacture complete x-ray microanalysis systems with video image collection and storage. The *TN-8500 Image Analysis System* features dedicated imaging hardware and software combined in an integrated system for advanced applications from the simplest particle size analysis to the most complex imaging applications such as fast Fourier transformation and 3-D reconstruction.

Carl Zeiss offer a family of upgradeable products including parallel processing software. The *Videoplan-Vidas-Ibas* line of digital image processing systems offers three different levels of automation. The *videoplan* takes advantage of the user's experience in recognizing complex structures. Measurements are performed by tracing contours with a cursor on a digitizing tablet or on a TV on-line image. The evaluation is supported by automatic data processing which includes data management. The *Vidas* system digitizes the images, which are then processed by *Ibas*. The *Ibas* system supports advanced procedures such as texture analysis and pattern recognition.

3.14.4 Confocal laser-scanning microscopy (CLSM)

In the CLSM a laser illuminates a pinhole that functions as a point light source. The divergent beam from this source is focused on the surface or

inside the particle to be examined. Reflected light from this location travels back to the lens, is focused and brought to the analyzer pinhole by means of a semi-transparent mirror and thence to a photomultiplier. By moving the illumination spot through the analyzed volume the complete particle can be registered in all three dimensions.

The method not only has the advantage of a three-dimensional registration of objects but also a considerable increased optical resolution. The *Leica CLSM* gives a lateral resolution of 0.25 μm .

(CLSM) has been used to generate three-dimensional information on particle size, shape and porosity [141]. The CLSM has been used to measure particle size distribution *in situ* and *ex situ* using computer based image analysis system [142]. A model was developed to assess processing conditions to produce a floc with desirable characteristics in an enhanced actinide removal. Ferreira *et al.* [143] present some additional methods of measuring wood pulp fibers and compares these with data from CLSM

3.14.5 On-line microscopy

On-line systems, covered more fully in Chapter 10, have been developed for measuring particle contamination in molten polymers [144] and for measuring particle size and shape. Microscopy is combined with a light-scanning device for particle size and shape determination in the Galai instrument. Castellini *et al.* [145] use a pulsed semiconductor laser as a light source to illuminate a flowing stream of particles, in the 2 to 400 μm size range, and determine their shape using a shadowgraph technique.

Herpfer and Jeng [146] used streak particle imaging velocimetry for planar measurement of droplet velocities and sizes. They encountered problems due to out-of-focus effects of the PIV imaging procedure.

Kato *et al.* [147] applied flow visualization and image processing to measure the velocity and size of glass beads of size, 50, 100 and 200 μm , falling through a pipe using a stereo-imaging technique.

Malot and Blaisot [148] determined particle size and sphericity of low density sprays by image analysis. Particle size distribution, in the 125 to 2000 μm size range, was determined by incoherent back-light imaging and shape by morphological analysis.

Blandin *et al.* [149] measured agglomeration in a crystallizer using a video camera focused on a thick black screen inside the crystallizer and connected to an image analysis system. This system films and measures particles circulating between the screen and the transparent crystallizer wall.

Danfoss QueCheck Vision System performs a continuous analysis directly from the production line, typically at 0.5 s intervals. The final results of the measurement are available after 100-300 frames so that an equivalent sieve analysis is completed every 3 min. The particle size distribution is documented via an interface with database and printer. The material is fed in a fine stream, by means of a vibratory feeder, past a vision camera that calculates the size distribution as it falls. The system has been applied to measuring the size distribution of sugar crystals. On-line image processing has also been applied to monitoring granule size distribution and shape in fluidized bed granulation [150].

3.14.6 Flatbed scanners

The size range of most CCD-based imaging systems does not exceed two orders of magnitude. A sensor array of 500 by 500 pixels does not give a correct reproduction of objects smaller than 4 by 4 pixels and any object greater than 500 pixels will be larger than the imaging area. Due to this limitation it is necessary to examine a large number of images for samples having a wide size distribution. Optical systems have the further limitation in that large objects are not in focus at the same magnification as small ones.

Flatbed scanners offer a large imaging area, usually 12 by 8 inches, an optical resolution of at least 300 pixels per inch and grayscale or color imaging. Scanner images therefore contain far more information than images from a CCD camera. A black and white full page image at 1200 ppi is equivalent to 500 images taken with a 500 by 500 pixel camera. However optical magnification is not possible and this limits the scanner to a size range of two orders in magnitude. This system is particularly suitable to determine the size and shape of fragile agglomerates of irregular shape with a wide range of sizes [151].

3.14.7 Dark field microscopy

DFM is considered to be the most sensitive light microscope method. The light is directed through an outer ring on to a mirror (Figure 3.11) and reflected on to the surface. An object on the surface will reflect light back into an inner tube and focused with a lens to the observer. If the surface is clean the rays are reflected back into the outer ring and the surface looks dark. Best results are obtained using sample carriers with a flat polished surface.

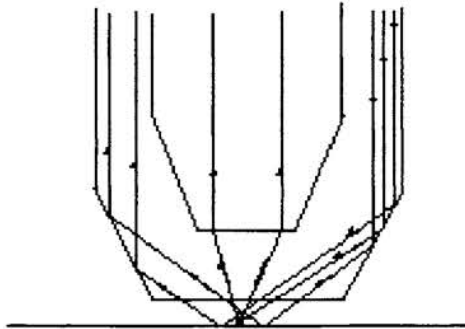


Fig. 3.11 Paths of rays in dark field microscopy

To get information about the lowest detection limit Schmidt *et. al.* [152] carried out experiments using monosize, spherical, fluorescent particles of known diameter. They deposited the particles on a wafer surface and observed them with a fluorescent and DFM. With both methods the light off the particles was detected and the sub- μm particles appeared larger than using a usual light microscope with a lower detection limit of $0.08 \mu\text{m}$.

Schmidt *et. al.* [153] investigated the use of dark field microscopy (DFM) to measure fibrous particles. Large areas were examined for statistical reliability. A high correlation was found between DFM and light microscopy for fiber lengths greater than $1 \mu\text{m}$.

3.14.8 Phase contrast microscopy

In phase contrast microscopy particles are sampled on to a membrane filter that is treated with acetone and glycerin triacetate to make the filter transparent. Problems associated with the preparation step, and low depth of focus limit thus the applicability of the method [153].

3.14.9 Polarized light microscopy (PLM)

The morphology and size of high explosive crystal grains are known to affect their processing characteristics and shock sensitivity. Particle size distributions are normally obtained by light diffraction assuming a spherical model. PLM and SEM reveal this assumption to be incorrect. By combining PLM, SEM and LD a quantitative measure of size and morphology can be obtained. Mean sizes and aspect ratios are determined and refined to give best fit to LD data and a comparison made between these three procedures [154].

3.14 10 Dipix 1440F power scope imaging microscope

The 1440F is a fluorescent microscope, powered by a high intensity mercury arc lamp, coupled with a high speed image analyzer which was designed specifically for automatic image analysis of agriculture and food products. Certain molecules absorb energy when excited by high intensity radiation. The excited molecules emit a portion of the absorbed energy when returning to ground state. Two types of spectra are associated with molecules which fluoresce – excitation and emission. The spectra have characteristic shapes and wavelength maxima that are specific to the absorbing components. This unique “fingerprint” feature can be used for identification purposes.

3.14 11 Transmission wide field phase contrast microscopy

A phase contrast wide field transmission microscope combining the advantages of interferomic and confocal techniques has been developed [155]. Confocal operation is achieved by superimposing speckle illumination of a reference beam in a Mach-Zehnder interferometer with a matched speckle pattern of the object beam. The technique was applied to both dry powders and suspensions and gave good agreement with modelled results. Data acquisition time is less than a millisecond.

3.15 Electron microscopy

When a solid is bombarded with high energy electrons the interaction produces secondary electrons (elastic), back-scattered electrons (inelastic), low loss electrons, Auger electrons, photo electrons, electron diffraction, characteristic x-rays, x-ray continuum, light, hole electron pairs and specimen current. These interactions are used to identify the specimen and elements of the specimen and can also be used to physically characterize particulate systems.

Transmission electron microscopy (TEM) is used for very fine particles or thin specimens of crystalline materials. The elastically scattered electrons give amplitude contrast which is proportional to mass thickness. The inelastically scattered electrons suffer small energy losses and give high phase contrast. Bright field images form when electrons, which are inelastically scattered through small angles, combine with unscattered electrons, whereas dark field images are formed only from the scattered electrons. Scanning transmission electron microscopy (STEM) allows

simultaneous viewing of both images and this is one of its major advantages.

The skill level required to operate and prepare specimens for a TEM is significantly higher than that associated with a SEM [156].

For scanning electron microscopy (SEM) the two most important interactions are:

The generation of secondary electrons, which are the result of elastic collisions and typically less than 50 eV. The images formed by these are the most common and are marked by great depth of field.

Backscattered electrons, which are less applicable to particle sizing but have niche uses; the contrast is closely related to the atomic number of the sample and typically the voltage is greater than 50 eV.

3.16 Transmission electron microscopy (TEM)

TEM is used for the direct examination of particles in the 0.01 to 5 μm size range [157]. The TEM operates by flooding the sample with an electron beam, most commonly at 100-200 keV, and generating an image on a fluorescent screen or a photographic plate beyond the sample. Analyses can be performed directly on the screen images, but this ties down the instrument for long periods of time, hence it is more usual to analyze photographic images.

TEMs operate in the magnification range from about 600 \times to 1,000,000 \times . Many particle size studies can be carried out at magnifications of less than 4,000 \times and several relatively inexpensive instruments are available giving magnifications up to 10,000 \times . Resolution capability of the best instrument currently available is sub-0.2 nm for line-to-line and approximately 0.2 to 0.3 nm for point-to-point.

Calibration is usually effected with narrowly classified polystyrene lattices available from Dow Chemicals or Duke Scientific, but diffraction gratings are necessary for high accuracy work. Single crystals of stable, well-characterized materials such as gold may be used as diffraction gratings and lattice fringe imaging can give direct calibration. Absolute calibration is uncertain to within 5% [158].

Some TEMs have a closed circuit television system fitted so that the images can be fed directly to an automatic image analysis system.

3.16.1 Specimen preparation for TEM

Specimens for TEM are often deposited on or in a thin (10 to 20 nm) membrane that rests on a grid. These grids are usually made of copper and

form a support for the film, which is usually only self-supporting over a small area (Figure 3.12). Specialty grids are available from a number of suppliers to fit particular needs. Examples would be nylon or beryllium grids for special characterization needs, or locator grids with numbered and/or lettered field markers.

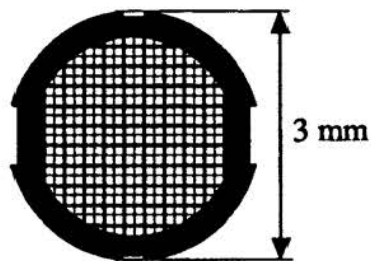


Fig. 3.12 Electron microscope grid.

Since most materials are opaque to the electron beam, even when only a few hundred nanometers thick, special problems arise in the production of suitable mounted specimens. Specimen support films are usually made of plastic or carbon, though other materials have also been used. Suitable film solutions may be made up of 2% w/v formvar (polyvinyl formal) in ethylene dichloride or chloroform.

Films may be produced in the following manner [159,160]. A dish about 20 cm in diameter is filled with clean distilled water and a large circle of 200-mesh steel gauze is placed on the bottom of the dish. A number of grids are placed on the wire gauze, then two drops of the film solution are dropped on to the surface of the water and the film that results after the solvent has evaporated is removed with a needle; this ensures that the water surface is clean. A second film, formed the same way, is removed by raising the wire gauze containing the grids that are then allowed to dry. A pre-examination of the grids in the electron microscope is desirable as this enables dirty films to be rejected, and the film polymerizes in the electron beam, thus greatly increasing its strength.

An alternative procedure is to clean a microscope slide with detergent and polish with a clean cloth without rinsing away the detergent, so as to form a hydrophilic layer at the surface, which facilitates stripping. The slide is dipped in a solution of formvar in ethylene dichloride (0.3% to 0.7% depending on the film thickness required) and allowed to drain dry. The film may be floated on to a water surface and mounted on grids as before. If individual grids are required, the film may be cut into small

squares with a needle or razor blade. The mounting operation is easier if a special jig is used [161]. The jig is a brass cylinder about 1 in. long and 0.5 in. diameter with a hole of the same diameter as the specimen drilled and tapped through its axis. A set-screw in the threaded hole is adjusted so that its end is flush with the face of the plug and withdrawn slightly to leave a shallow recess. The specimen grid is held in this recess and the membrane is lifted from the water surface with a wire loop of slightly larger diameter than the jig, surplus water being carefully removed with blotting paper. The wire loop is then lowered over the jig and, when the membrane is dry, the grid is raised by means of the screw, surplus membrane being removed by scoring round the grid with a needle. Special apparatus has also been described for producing plastic films of uniform thickness suitable for the preparation of replicas [162].

Carbon films are prepared under vacuum (10-3 mmHg) by electrical discharge from two pointed hard graphite rods [163]. Films are best deposited on microscope slides cleaned with detergent and placed about 10 to 15 cm from the source. A thickness indicator, consisting of a drop of vacuum oil on a piece of white glazed porcelain, is placed beside the slide. During the discharge, the porcelain not covered with oil takes on a brownish color, changing to a light chocolate shade as the film thickness increases from 5 to 10 nm, the latter being a suitable thickness for general use. Evaporation is completed in about half a second with a current of 50 A. The film may then be floated on to the surface of distilled water and picked up as a whole or scored into small squares. A simple method of producing a suitable specimen is to place a few milligrams of the powder on a microscope slide, add a drop of 1% to 2% w/v suspension of formvar in a suitable solvent and rub out the slide with a glass rod. Further solvent is added if required and the dispersion is spread over the slide and allowed to dry. The film is removed from the slide and mounted on the grid as before.

Another method of preparing the sample is to disperse it in linseed oil, which is then thinned with white spirit. The dispersion is spread over a microscope slide that is immersed in white spirit for a few minutes to remove the oil. After drying the slide a thin layer of carbon is deposited on the specimen to form a supporting film. Finally this is floated off on water as before and picked up on a grid for examination [91].

A dispersed sample may also be obtained by means of an aerosol sampling device. A suitable technique is to form a sandwich of plastic film particles and 20 nm thick carbon. The underlying plastic may then be washed away with solvent and the specimen examined after shadowing [159,160,162].

A suspension of the powder may be made up and a drop placed on a grid by means of a pipette or hydrometer syringe. However, this often produces an uneven deposit. Spraying the suspension on to the grid often produces a more uniform deposit; several suitable spray guns have been described [157,164].

Timbrell [82] modified the Hamilton and Phelps [165] method for the preparation of transparent profiles to facilitate electron microscopy. The metal film is floated on to a water surface and picked up on a grid. In cases of difficulty, the slide is first dipped into 1% hydrofluoric acid to release the edge of the film and the process is completed in water. Although the metal film is strong enough to be floated off whole, it is preferable to score it into small squares as described earlier and then remove the separate pieces. In order to obtain reliable results for particle size analysis, as many separate grids as possible should be prepared and a large number of electron micrographs taken from each. Many other methods have been used and the preparation of the particle dispersion is the most important aspect of sizing by electron microscopy.

In an analysis of the errors involved in electron microscopy, Cartwright and Skidmore [166] examined the optical microscopy specimens produced by thermal precipitation. The specimens were then stripped from the microscope slides and the fines were counted, using an electron microscope. Good agreement was obtained by examining 1000 particles in the electron microscope using about 60 fields of view (60 micrographs) and almost 4000 particles in the optical microscope. To obtain accurate magnification calibration, four overlapping micrographs along the bar of a readily identifiable grid square were taken and the total length of the image of the grid bar was measured from the micrographs directly, using an optical microscope.

The surface areas of dust samples as determined by optical and electron microscope have also been compared [167]. Pore size distributions of thin films of Al_2O_3 , as measured by TEM, have also been compared with those determined by gas adsorption/desorption [168]. It has also been suggested that electron microscope gives a truer estimate of surface area than gas adsorption techniques [169]. Further information can be obtained in a recent review of specimen preparation for TEM [170].

Two other effects, which may influence apparent particle size, relate to the effect of the flooding electron beam on the particles. One of these is charging of non-conducting particles, which spreads the beam around the particles and makes sharp focusing impossible. The other is the gradual accumulation of vacuum pump oil (and other things) on the charged sample in the sample chamber. This often appears as a slowly developing skin

around the particle thus increasing its apparent size. A view at reduced magnification will reveal a discolored region. This effect limits the time one can spend in a particular field of view, but the contamination is usually slow enough to not seriously jeopardize the study. The higher vacuum systems found in newer instruments reduces this effect.

3.16.2 Replica and shadowing techniques

Replicas are thin films of electron-transparent material that are cast on opaque specimens in order that their surface structure may be studied. The basic procedure is to form a film on the substance to be examined, separate the two and examine the film. If a reverse of the original is unsatisfactory, a positive replica may be obtained by repeating the process. One method is to deposit the specimen on a formvar-covered grid, vacuum-deposit about 10nm of carbon, remove the formvar by rinsing with chloroform and finally remove the specimen with a suitable solvent [171]. Instead of a backing film, it is sometimes possible to prepare a carbon replica of a dried suspension deposited on a microscope slide, the replica being washed off the slide in a water bath or a bath of hydrofluoric acid. The carbon film may be strengthened immediately after being deposited by dipping the slide in a 2% w/v solution of Bedacryl 122X in benzene, which is removed by a suitable solvent after the film has been deposited on a grid range [157]. Numerous variations of these techniques have been used [32,67,160,172-174].

In order to determine surface characteristics and particle thickness, it is usual to deposit obliquely a film of heavy metal on to a specimen or its replica. The metal is applied by deposition in a hard vacuum by a small source in order that a nearly parallel beam may reach the specimen. The technique was originated by Williams and Wyckoff [175] in 1946 and has been used extensively since.

Surface topography can also be studied using 3-D imaging. Two successive photographs of the same field are made with the specimen tilted by 11° to 14° between photographs. This stereo-pair can then be viewed with stereo viewing lenses for a remarkable sense of the third dimension.

3.16.3 Chemical analysis

When particles are bombarded with electrons, they emit radiation that depends upon their chemical composition. The Auger process [176,177] is a secondary electron process that follows the ejection of an electron from an inner shell level. The hole is filled by an electron falling to the vacant

level, which provides the energy for another electron to be emitted. The energy of this Auger electron is characteristic of the molecule involved. The process can be studied by using monochromatic or polychromatic radiation or electron beams. There have been many studies on metal surfaces using vacuum ultra violet techniques and the energy distribution curves (EDCs) obtained give information on the band structure of the metals.

The use of soft x-rays is known as electron spectroscopy for chemical analysis (ESCA), or x-ray photo-electron spectroscopy (XPS). In addition to ejecting electrons from the valence shell orbits, the x-rays have sufficient energy to eject electrons from some of the inner shells. These are essentially atomic in nature and the spectra produced are characteristic of the atom concerned, rather than the molecule of which it forms a part [178].

These, and other techniques, may be applied in electron microscopy to permit chemical assay and particle size analysis to be run concurrently [179].

3.17 Scanning electron microscopy

In SEM a fine beam of electrons of medium energy (5-50 keV) is caused to scan across the sample in a series of parallel tracks [180]. These electrons interact with the sample, producing secondary electron emission (SEE), back-scattered electrons (BSE), light cathodoluminescence and x-rays. Each of these signals can be detected and displayed on the screen of a cathode ray tube like a television picture. Examinations are generally made on photographic records of the screen, although the images can be processed on-line [181]. The SEM is considerably faster and gives more three-dimensional detail than the TEM.

Some instruments can take samples as large as 8 in. square and parts viewed at magnifications varying from 20× to 100,000× at resolutions of 5 to 7 nm. The latest instruments are capable of resolutions down to 0.7 nm. The depth of focus is nearly 300 times that of the optical microscope. Because of its great depth of focus the SEM can give considerable information about the surface texture of particles.

In both the SEE and BSE modes, the particles appear as being viewed from above. In the SEE mode the particles appear to be illuminated diffusely, and particle size and aggregation behavior can be studied but there is little indication of height. In the BSE mode the particles appear to be illuminated by a point source of light and the resulting shadows give a good indication of height. Several of the current methods of particle size analysis can be adapted for the measurement of images in SEM

photographic records. There is also active interest in the development of analysis techniques that will make use of the three-dimensional image presentation.

Many of the image modification procedures associated with automatic image analysis are applicable also with images based on back-scattered electrons. This permits thresholding, classification, boundary enhancement, separation of touching particles, etc. to be carried out before the image is measured [182]. There are three ways of producing a stereographic image in an SEM: horizontally shifting the object, tilting the object and tilting the electron beam. The first is the method used for stereography of aerial photographs, though it is the viewpoint that shifts in this case. The second method suffers the defect that it is difficult to position the object accurately after tilting. Kolendik [183] examined both these methods and preferred the former whereas Kramarenko [184] stated that the first method was more effective and easier for high accuracy measurement. The tilting method has been described by Shoji *et. al.* [185]; essentially it generates a binocular image by striking the specimen at oblique angles.

ASTM provides standard reference materials for calibrating SEM's: SRM 484 g can be used to calibrate the magnification in the range 1000× to 20,00×, SRM 2090 is a new standard made of a silicon chip with well-defined line separations and SRM 2069b is a standard of graphitized rayon fibers. ASTM E766-98 [186] discusses standard practice for calibrating the magnification of an SEM.

Le Mont Scientific B-10 system features an energy-dispersive x-ray detector. Particles are loaded and interrogated to find size and shape; various software options are available. The Bausch and Lomb system has also been applied to electron beam microscopy [187,188]. *Tracor Northern* describe an integrated system for the collection and processing of analytical and image data from SEM and STEM [189,190]. Various sample preparation methods have been described.

Krinsley and Margolis [191] mounted sand grains in Duco cement on the SEM target stub; this technique is not suitable for size analysis and cannot be used for fine particles [192]. Willard and Hjelmstad [193] tried to improve this technique, in order to mount fine coal, by using double-backed adhesive tape. They had limited success with particles smaller than 30 μm and found that the method was unsuitable for larger particles. White *et. al.* [194] prepared specimens of alumina by aspirating droplets of alumina suspension in NH₄OH solution on to aluminized glass slides and the fixing the slides to the SEM stub. This procedure is very slow and has been criticized as being unsuitable for particles which readily agglomerate

or which swell in aqueous solutions. Turner *et al.* [192] prepared an adhesive layer by immersing about 3 ft. of Scotch Tape in 150 cm³ of carbon tetrachloride or chloroform, agitating long enough for the adhesive layer to be dissolved and then removing the tape. A few drops of the solution were deposited on the SEM stub, the thickness of the adhesive layer on the stub being controlled by adjusting the concentration and the number of drops applied. A suitable amount of powder was dispersed in acetone (0.5% w/v) and a drop taken on a glass rod and dropped on to the stub. The mounted specimen was then coated with a 15 nm layer of aluminum. They also describe a method for studying agglomerates by freeze drying. Once the images are recorded, the quality of the analysis depends on the quality of the particle dispersion, the contrast and focus (sharpness of image). From this point on, the particle sizing proceeds as in the optical process described earlier. King and Schneider [195] state that the available commercial image processing and image analysis software systems do not usually include adequate algorithms for the effective analysis of multi-phase mineralogical textures. Filtering algorithms are usually inadequate for the accurate removal of image noise without compromising the integrity of phase edges. Although most systems offer good algorithms for the analysis of binary images, algorithms for higher order images are almost non-existent and these are essential for mineralogical analysis. They describe the development of an image analysis system that overcomes these limitations. It is based on SEM equipped with secondary electron and back-scattered electron detectors, an image memory for the storage of digital images captured at slow scan speeds and a SUN workstation for image processing and image analysis.

A scanning electron microscope connected to an image processor allows one to obtain, automatically, a wide variety of parameters describing the shape and granulometric properties of powder particles. This method offers numerous advantages over other methods with automatic and numerous measurements with a saving in time and yielding more accurate data with a smaller number of observations [196]. Particle size and shape have been determined using a special computer program that was based on obtaining a pixel matrix of the particle boundary by the digitizing of the particle image [197] It was concluded that fractal analysis is a useful tool for correlating the fractal parameter with the physical description and flow properties of pharmaceutical solids.

3.18 Other scanning electron microscopy techniques

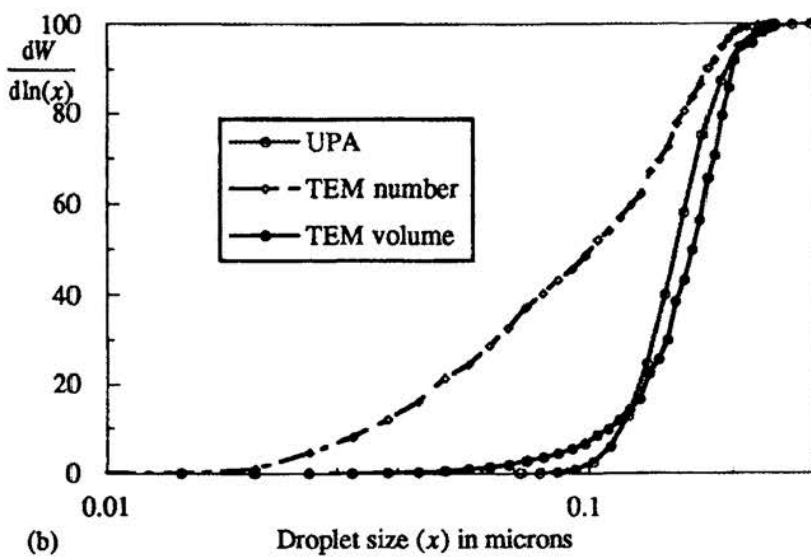
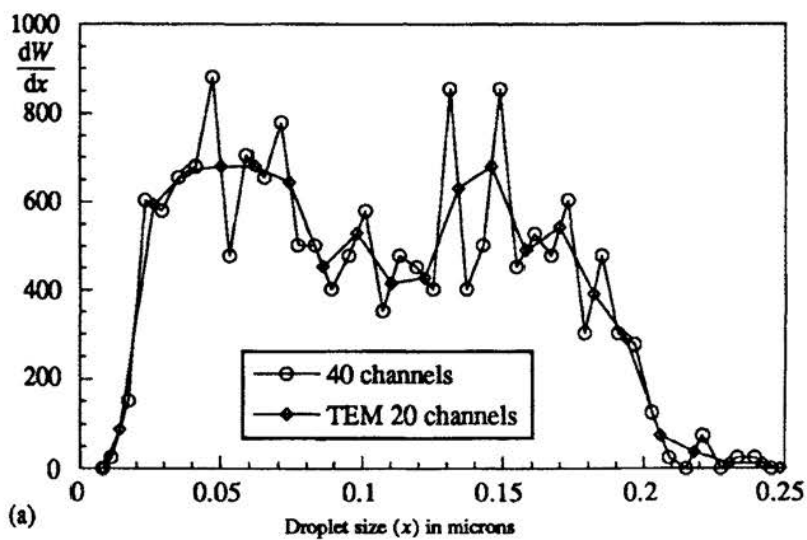
The scanning transmission electron microscope (STEM) uses a fine beam of electrons to scan the specimen as with the SEM, but detects transmitted electrons for display on a cathode ray tube (CRT). The performance is similar to the TEM, but with certain advantages. Since the sample is irradiated with a scanning beam, there is less beam damage to sensitive samples. In addition, for easily damaged samples, focusing can be done on a small region of the sample and instantly "transplanted" to an undamaged part for image recording. The CRT display of the image usually gives more flexibility in manipulating data, transforming it and so on. Use of the annular dark field detector also allows simultaneous bright field and dark field imaging of the same sample field.

Additional advantages enjoyed by the dedicated STEM units are their clean, high vacuum systems in use and their very bright electron source in the field emission gun. The high vacuum (10^{-11} torr in the gun chamber and 10^{-8} to 10^{-9} torr in the sample chamber) allows prolonged observation of the sample without contamination, and the bright source allows viewing of data collection at TV scan rates.

The scanning tunneling electron microscope (STM), invented in 1981, allows examination of non-conductive surfaces [198] down to atomic resolution and can operate in ambient and aqueous environments [199,200]. Early references to the instrument use the acronym STEM, which produced confusion with the scanning transmission electron microscope. More recently, the consensus has been to use STM, as the acronym for the tunneling instrument.

Since the introduction of the STM a number of variations have been devised, such as ATM (atomic force microscope). The basic concept is that piezoelectric actuators move a miniature cantilever arm (with a nm-sized tip) across the sample while a non-contact optical system measures the deflection of the cantilever caused by atomic scale features. The deflection is proportional to the normal force exerted by the sample on the probe tip and images are generated by raster scanning the sample [201]. One application of this technique was to measure the thickness and size distribution of sub-micron clay particles with diameters in the 0.1 to 1 μm size range and thickness from 0.01 to 0.12 μm [202].

MFM (magnetic force microscope), LFM (lateral force, or friction force microscope), etc. None of the above finds wide use for particle size determination. The AFM has however been used to determine the shape, size and types of particle on a polished silicon wafer surface [203].



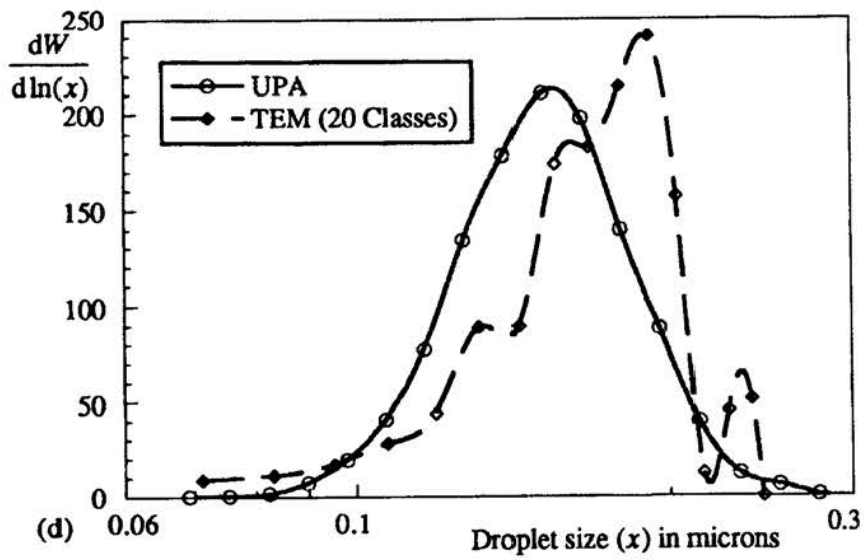
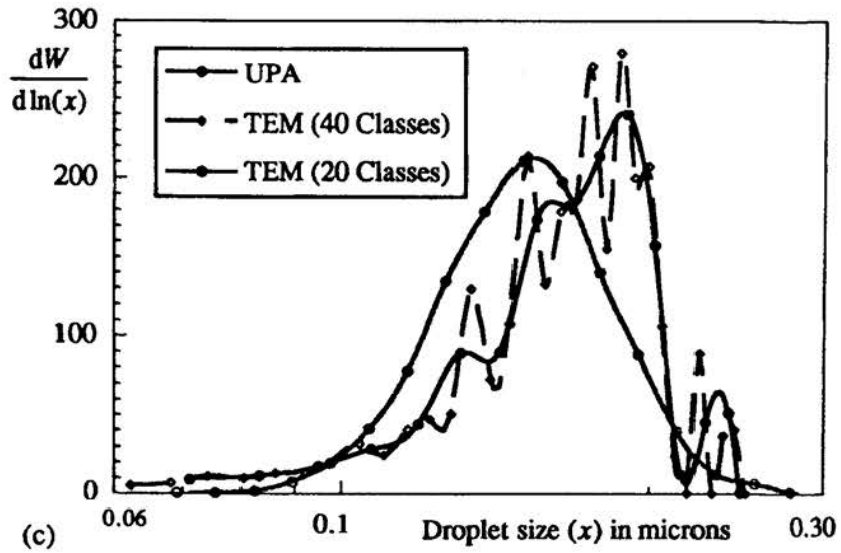


Fig. 3.13 Presentation and interpretation of microscope data.

and STM have been applied to nanoparticles and these studies have demonstrated that the techniques have potential for very small particles [204-206]. While atomic resolution is not possible with AFM; STM showed atomically resolved clusters on supports in some cases. An interesting feature of STM is scanning tunneling spectroscopy which can be used to distinguish between metals and semiconductors and to measure the band gap of the latter [207]. A detailed review of the capabilities of these technique has been published by Springer [208]. TEM and SEM are sometimes unable to clearly differentiate between agglomerates, particles and grains in soil samples and sample preparation is difficult and tedious. ATM has been used to overcome these limitations with a sample of sub-micron oxisol. The thickness and diameter of soil particles deposited in freshly cleaved mica were measured for each individual particle. Assuming cylindrical shape and a constant density the mass particle size distribution was obtainable [209].

3.19 Errors involved in converting a number to a volume count

This example consists of TEM number count data on 662 droplets in 40 size classes linearly spaced between 0.015 μm and 0.250 μm . The resulting number distribution is noisy (Figure 3.13a) due to the large number of size classes and the linear presentation of what is essentially a log-normal distribution.

The conversion to a volume distribution and comparison with Microtrac UPA data are shown in Figure 3.13b. The poor agreement is due, in part, to the errors generated when converting a number distribution of a wide-ranging population into a volume distribution. A single 0.25 μm droplet has the same volume as 4630 droplets of size 0.015 μm hence over-counting by a single large particle is equivalent to over-counting 4630 small particles.

Reducing the number of classes to 20, and plotting logarithmically, greatly reduces the noise (Figure 3.13c).

Comparison between UPA and TEM data (Figure 3.13d) illustrates that the difference between the two sets of data is due to overcounting large particles in the TEM analysis. This error occurs when all droplets in the photomicrograph are counted. It is essential that droplets overlapping two adjacent boundaries be neglected since the probability of large droplets overlapping is greater than the probability for small droplets. This example illustrate four points:

1. Number distributions, for powders having a wide size range, should never be converted into volume distributions unless a statistically acceptable number of particles in the largest size category have been counted. For a microscope count, the correct procedure for carrying out a size distribution by weight should be followed.
2. Dividing the distribution into too many size categories can result in a noisy distribution unless sufficient particles are measured. The size ranges should be arranged logarithmically for powders having a wide size range.
3. When sizing photomicrographs, a frame should be drawn in the photograph, displaced from the edge by a distance equal to the radius of the largest particle in the distribution. All particles overlapping two adjacent sides of the frame should be left uncounted, otherwise the large particles are over-counted.

Data should be presented in such a way as to highlight the required information. Incorrect presentation can completely hide relevant information

3.20 Evaluation of procedures

Several alumina powders have been analyzed using SEM, TEM, gas adsorption, x-ray Sedigraph and laser light scattering and the results compared [210].

References

- 1 Schmidt, F., Schmidt, K.G. and Fissan, H. (1990), *J. Aerosol Sci.*, **21**, Suppl. 1, S535-S538, 142
- 2 McCrone, W.C. (1991), *Phys. Meth. Chem.*, 2nd ed., eds. B.W. Rossiter and J.F. Hamilton, Wiley, N.Y., 142
- 3 Mayette, D.C., McMahon, B. and Daghlain, C.P. (1992), *Ultrapure Water*, **9**(4), 20, 22-24, 26-29, 32-34, 142, 147
- 4 Sutherland, D.N. (1993), *Part. Part. Syst. Charact.*, **10**(5), 271-274, 142
- 5 Lane, G.S. and Richmond, G.D. (1993), *Proc. 18th Int. Min. Proc. Cong.*, Sydney, 897-904, 142
- 6 Welford, G. A. (1960), *Optics in Metrology*, 85, 143
- 7 Groen, F.C.A., Young, I.T. and Ligthart, T. (1985), *Cytometry*, **6**(81), 144

- 8 Kenney, L.C. (1985), *Particle Size Analysis*, 247-260, Proc. 5th International Conf., Analyt. Div. Chem. Soc., ed. P.J. Lloyd, publ. John Wiley & Sons, 144
- 9 ASTM D4791-898 (1989), *Standard test method for flat and elongated particles*, 144
- 10 Broyles, D.A., Rimmer, H.W. and Adel, G.T. (1996), *Kona*, **14**, 130-138, 144
- 11 BS 3406 Part 4 (1993), *Methods for determination of particle size distribution, Part 4, Guide to microscopy and image analysis methods*, 144, 146, 154, 155, 162
- 12 ASTM E20 *Practice for particle size analysis of particulate substances in the range 0.5 μm to 75 μm* , 144
- 13 ASTM E175-82 (1995), *Standard terminology of microscopy*, 144
- 14 ASTM E766-98 (1998), *Standard practice for calibrating the magnification of an scanning electron microscope*, 144
- 15 NF 11-661 *Test methods for particle size analysis-Determination of particle size of powders-Optical microscope*, 144
- 16 NF X11-696 *Test methods for particle size analysis through image analysis*, 144
- 17 ISO/CD 13322 (Draft Standard), *Particle size analysis-Image analysis methods*, 145
- 18 Hartman, A.W. (1984), *Powder Technol.*, **39**, 49, 145
- 19 Hartman, A.W. (1985), *Powder Technol.*, **42**, 259, 145
- 20 Hartman, A.W. (1986), *Powder Technol.*, **46**, 109, 145
- 21 Wilson, R. and Elkington, A.A. (1985), *Int. Conf. Royal Soc. Chem. Particle Size Analysis Group*, 261-270, ed. P.J. Lloyd, publ. John Wiley & Sons, 145, 170
- 22 National Physical Laboratory. *Reference Stage Graticule for Image Analysis calibration*, Teddington, Middlesex, U.K., 145, 170
- 23 Charman, W.N. (1961), *Ph.D. thesis*, London Univ., 146, 147
- 24 Rowe, S.H. (1955), *Microscope*, **15**, 216, 147
- 25 Humphries, D.W. (1961), *J. Sediment. Petrol.*, **31**, 471-473, 148
- 26 Hawkins, A.E. (1993), *The Shape of Powder Particle Outlines*, 22, John Wiley & Sons, 148
- 27 Hawkins, A.E. and Davies, K.W. (1984), *Part. Part. Syst. Charact.*, **4**, 22-27, 148
- 28 Cairncross, A., Flaherty, D.M. and Klabunde, U. (1993), *Proc. Microsc. Soc. of America*, 51st A.G.M., August, Cincinnati, Ohio, 148
- 29 Allen, T. (1994), *Powder Technol.*, **79**, 61-68, 148
- 30 Green, M. (1921), *J. Franklin Inst.*, **192**, 657, 148
- 31 Dunn, E. (1930), *Ind. Engg. Chem., Analyt. Ed.*, **2**, 59, 148
- 32 Orr, C. and Dallevale, J.M. (1959), *Fine Particle Measurement*, Macmillan, N.Y., 148, 156, 192
- 33 ASTM (1976), *Annual Book of Standards, Part 4. Particle Size Measurement, Microscopy*, E20-69, Reapproved 1984, 148

- 34 Dullien, F.A.L. and Mehta, P.N. (1972), *Powder Technol.*, **5**, 179-194, 149
- 35 Harwood, M.G. (1954), *Brit. J. Appl. Phys.*, Suppl. 3, S193, 149
- 36 Allen, R.P. (1942), *Ind. Engg. Chem.*, Analyt. Ed., **14**, 92, 149
- 37 Lenz, F. (1954), *Optik*, **11**, 524, 149
- 38 Ellison, McK. (1954), *Nature*, **173**, 948, 149
- 39 Green, M. (1946), *Ind. Engg. Chem.*, **38**, 579, 149
- 40 Pidgeon, F.D. and Dodd, C.G. (1954), *Analyt. Chem.*, **26**, 1823-1828, 149
- 41 Rosinski, J., Glaess, H.E. and McCulley, C.R. (1956), *Analyt. Chem.*, **28**, 486, 150
- 42 Timbrell, V. (1972), *J. Appl. Phys.*, **43**(11), 4839, 150
- 43 Timbrell, V. (1973), *Microscope*, **20**, 365, 150
- 44 McCrone, W.C. (1970), *Microscope*, **18**(1), 1, 150
- 45 Delly, J.G. (1989), *Microscope*, **18**, 205-211, 150
- 46 Proctor, T.D. and Harris, G.W. (1974), *J. Aerosol Sci.*, **5**(1), 81-90, 150
- 47 Proctor, T.D. and Barker, D. (1974), *J. Aerosol Sci.*, **5**(1), 91-99, 150
- 48 Anon, *Ceram. Age*, Dec., 150
- 49 Amor, A.F. and Block, M. (1968), *J. Royal Microsc. Soc.*, **88**(4), 601-605, 150
- 50 Hamilton, R.J. and Phelps, B.A. (1956), *Brit. J. Appl. Phys.*, **7**, 186, 150
- 51 Eckoff, R.K. and Enstad, G. (1975), *Powder Technol.*, **11**, 1-10, 151
- 52 Dullien, F.A.L., Rhodes, E. and Schroeter, S.R. (1969/70), *Powder Technol.*, **3**, 125-135, 151
- 53 Barberry, G. (1974), *Powder Technol.*, **9**(5/6), 231-240, 151
- 54 Sahu, B.K. (1976), *Powder Technol.*, **13**, 295-296, 151
- 55 Dullien, F.A.L. and Mehta, P.N. (1972), *Powder Technol.*, **5**, 179-194, 151
- 56 Dullien, F.A.L. (1973), *Am. Chem. Soc. Div. Org. Coat. Plast. Chem.*, Paper 33, **2**, 516-524, 151
- 57 Dullien, F.A.L. and Dahwan, G.K. (1974), *J. Colloid Interf. Sci.*, **47**(2), 337-349, 151
- 58 Nicholson, W.L. (1976), *J. Microsc.*, **107**(3), 323-324, 151
- 59 Saltzman, W.M., Pasternak, S.H. and Langer, R. (1987), *Chem. Eng. Sci.*, **42**(8), 1989-2004, 151
- 60 Martin, G. *et al.* (1923), *Trans. Ceram. Soc.*, **23**, 61, 1926, *Trans. Ceram. Soc.*, **25**.51.(1928), *Trans. Ceram. Soc.*, **27**, 285, 152
- 61 Heywood, H. (1946), *Trans. Inst. Min. Metall.*, **54**, 391, 136, 152
- 62 Feret, R.L. (1931), *Assoc. Int. pour l'essai des Mnt*, **2**, Group D, Zurich, 136, 152
- 63 Tomkoeff, S.L. (1945), *Nature*, **155**, 24, 152
- 64 Moran, P.A.P. (1944), *Nature*, **154**, 490, 152
- 65 Steinheitz, A.R. (1946), *Trans. Soc. Chem. Ind.*, **65**, 314, 152
- 66 Walton, W.H. (1948), *Nature*, **162**, 329, 153
- 67 Herdan, G. (1960), *Small Particle Statistics*, p140, Butterworths, 153, 192
- 68 Cauchy, A. (1840), *C.R. Acad. Sci.*, Paris, **13**, 1060, 154
- 69 Watson, H.H. (1936), *Trans. Inst. Min. Metall.*, **46**, 176, 154
- 70 Fairs, G.L. (1943), *Chem. Ind.*, **62**, 374-378,, 154

- 71 Fairs, G.L. (1951), *J. Royal Microsc. Soc.*, **71**, 209, 155
- 72 Watson, H.H. (1952), *Br. J. Ind. Med.*, **19**, 8, 155
- 73 May, K.R. (1965), *J. Scient. Instrum.*, **22**, 187, 155
- 74 Guruswamy, S. (1967), Particle Size Analysis Conf., *Soc. Analyt. Chem.*, 29-31, 156
- 75 Aschenbrenner, B.C. (1955), *Photogrammetric Engng.*, **21**, 376, 156
- 76 Hamilton, R.J. and Holdsworth, J.F. (1954), *Br. J. Appl. Phys.*, Suppl. 3, S101, 156
- 77 Heywood, H. (1946), *Bull. Inst. Min. Metall.*, No. 477, 488, 156
- 78 Watson, H.H. and Mulford, D.F. (1954), *Brit. J. Appl. Physics*, Suppl. 3, S105, 157
- 79 Fairs, G.L. (1954), Discussion, *ibid*, S1081, 157
- 80 ASTM (1951), E20-SIT, 1539, 157
- 81 Hamilton, R.J., Holdsworth, J.F. and Walton, W.H. (1954), *Br. J. Appl. Phys.*, Suppl. 3, S101-S105, 157, 166, 190
- 82 Timbrell, V. (1973), *Harold Heywood Memorial Symposium*, Loughborough Univ., England, 157
- 83 Nathan, I.F., Barnet, M.I and Turner, T.D. (1972), *Powder Technol.*, **5**(2), 105-110, 157
- 84 Vigneau, E., Loisel, C., Devaux, M. F. and Cantoni, P. (2000), *Powder Technol.*, **107**(3), 243-250, 159
- 85 Masuda, H. and Iinoya, K. (1971), *J. Chem. Engg.*, **4**(1), 60, 162
- 86 Jillavenkatesa, A., Dapkunas, S.J. and Lum, L-S. H. 2001, Particle Size Characterization, *National Institute of Standards and Technology, Sp. Publ.* 960-1, 162
- 87 Endter, F. and Gebauer, H. (1956), *Optik*, **13**, 87, 164
- 88 Duncan, A.A. (1974), *Report MH SMP-74-119F*, Dept. NTIS, Chicago, USA, 7pp., 164
- 89 Exnor, H.E. and Linck, E. (1977), *Powder Metall. Int.*, **9**(3), 131-133, 164
- 90 Becher, P. (1964), *J. Colloid Sci.*, **19**, 489, 164
- 91 Crowl, V.T. (1961), Report No 291, *Paint Research Station*, Teddington, Middlesex, U.K., 164, 167, 191
- 92 Anon (1978), *Powder Metall. Int.*, **10**(2), 95, 164
- 93 Chatfield, E.J. (1967), *J. Scient. Instrum.*, **44**, 615, 164
- 94 Lark, P.D. (1965), *Microscope*, **15**, 1-6, 166
- 95 Dyson, J. (1959), *Nature*, **184**, 1561, 166
- 96 Dyson, J. (1960), *J. Opt. Soc. Amer.*, **50**, 254-257, 166
- 97 Dyson, J. (1961), *AEI Engng.*, **1**, 13, 166
- 98 Payne, B.O. (1964), *Microscope*, **14**(6), 217, 166
- 99 Timbrell, V. (1952), *Nature*, **162**, 329, 166
- 100 Barnett, M.I. and Timbrell, V. (1962), *Pharm. J.*, 379, Oct., 166
- 101 Perry, R.W., Harris, J.E.C. and Scullion, H.J. (1977), *Particle Size Analysis, Conf. Proc.*, 18-30, *Analyt. Chem. Soc.*, Salford. U.K., ed. M.J. Groves, publ. Heyden, 166

- 102 BS 3625 (1963), Recertified (1994), *Specifications for eyepieces and stage graticules for the determination of the particle size of powders*, 166
- 103 Nichols, G. (1997), *Part. Part. Syst. Charact.*, **14**, 306, 166
- 104 Walton, W.H. (1954), *Br. J. Appl. Phys.*, suppl. 3, S121, 167
- 105 Vick, F.A. (1956), *Sci. Progr.*, **94**(1766), 655, 167
- 106 Morgan, B.B. (1967), *Research*, **10**, 271 London, U.K., 167
- 107 Taylor, W.K. (1954), *Brit. J. Appl. Phys*, suppl. 3, S156, 167
- 108 Roberts, F. and Young, J.Z. (1952), *Nature*, **169**, 962, 167
- 109 Bell, H.A. (1954), *Br. J. Appl. Phys.*, suppl. 3, 156, 167
- 110 Causley, D. and Young, J. (1955), *Z. Res.*, **8**, 430, 167
- 111 Mullard Film Scanning Particle Analyzer, *Mullard Tech. Leaflet.*, 167
- 112 Hawksley, P.G.W. (1954), *Br. J. Appl. Phys.*, suppl. 3, S125-S132, 167
- 113 *Casella Automatic Particle Counter and Sizer*, (Booklet 906A) Cooke, Troughton and Simms Ltd., 167
- 114 Allen, T. and Kaye, B.H. (1965), *Analyst*, **90**, 1068, 167
- 115 Fath, R., Enneking, U. and Sommer, K. (1986), *First World Congress Part. Technol.*, Nürnberg, 49, 170
- 116 Blackford, D.B. (1987), *Aerosol Sci. Technol.*, **6**, 85-89, 170
- 117 Smith, G.C. (1986), *NPL News*, (National Physical Lab.), **365**, 17, Teddington, Middlesex, U.K., 171
- 118 Smith, G.C. (1986), *NPL News*, (National Physical Lab.), **365**, 17, Teddington, Middlesex, U.K., 171
- 119 Issoukis, M. (1986), *Nature*, **322**, 91, 171
- 120 Issoukis, M. (1987), *Tappi J.*, **70**, 15, 171
- 121 Anon, Digital Image Analysis of Materials, *Outokompu Tech. Bull.*, 172
- 122 Gonzales, R.C. and Wintz, P. (1987), *Digital Image Processing*, 2nd ed., Addison-Wesley, 172
- 123 Weichert, R. (1992), *Image Analysis in Particle Technology*, Partec, 5th European Symp. in Particle Characterization, Nürnberg, Germany, **1**, 12, 173
- 124 Devaux, M.F., Roberts, P., Melcion, J.P. and Monredon, F. le. (1997), *Powder Technol.*, **90**(2), 141-147, 174
- 125 Davidson, J.A. (1993), *Part. Part.Syst. Charact.*, **9**(2), 94-104, 178
- 126 Serra, J. (1972), *J. Micro. Part I*, 93-103, 179
- 127 Serra, J. (1976), *cit 20*, 179
- 128 Serra, J. (1982), *Academic Press Inc.*, New York, 179
- 129 Matheron, G. (1972), *J. Micro. Part I*, **15**, 23, 179
- 130 Matheron, G. (1975), *Random Sets and Integral Geometry*, Wiley, New York, 179
- 131 Ma, X., Huang, T. and Yu, L. (1990), *Proc. World Congress Particle Technology*, Kyota, Japan Part I, 273-280, 179
- 132 Davidson, J.A., Etter, A.A., Thomas, T.R. and Butler, R.S. (1992), *Part. Part. Syst. Charact.*, **9**(2), 94-108, 179
- 133 Huller, D. (1984), *VDI-Fortschrittsberihite*, Reihe 3, Verfahrenstechnik, No 101, VDI-Verlag, Dusseldorf, 179

- 134 Wightman, C., Muzzio, F.J. and Wilder, J. (1996), *Powder Technol.*, **89**(2), 165-176, 179
- 135 Beck, M. and Sommer, K. (1995), *6th European Symp. Particle Charact., Partec*, Nürnberg, Germany, publ. NürnbergMesse, GmBh, 79-84, 179
- 136 Schäfer, M. (2002), *Part, Part, Syst, Charact.* **3**, 158-168, 180
- 137 Keeler, R. (1991), *Res. and Develop, Magazine*, March, 48-52, 181
- 138 Cohen, E.D. and Grotovsky, R. (1991), *44th Annual Conf. Soc. for Imaging Sci and Technol.*, St Paul Minn., 181
- 139 Davison, J.A. (1993), *Part. Part. Syst. Charact.*, **9**(2), 94-104., 182
- 140 Harrigan, K.A. (1996), *Cereal Foods World*, **41**, 593, 182
- 141 Bottlinger, M. and John, R. (1998), *Partec 98, 7th Europ. Symp. Particle Charact.*, 715-722, NürnbergMesse, MesseCentrum, Germany, 184
- 142 Hildred, K.L., Townson, P.S., G.V. and Williams, R.A. (2000), *Powder Technol.*, **108**(2-3), 164-172, 184
- 143 Ferreira, P.J., Vaz, M.H. and Figueiredo, M.M. (2002), *World Congress Particle Technology 4*, Sydney, Australia, July, 184
- 144 Kilham, L.B. (1987), *Tappi J.*, **70**, 156, 184
- 145 Castellini, C., Francini, F., Langobardi, G. and Papoloni, E. (1993), *Part. Part. Syst. Charact.*, **10**(5), 7-10, 184
- 146 Herpfer, D.C. and Jeng, S. (1997), *AIAA J.*, **35**, 127, 184
- 147 Kato, H., Nishino, A. and Torii, K. (1995), FED-V01, 209, *ASME*, New York, 115-122, 184
- 148 Malot, H. and Blaisot, J-B. (2000), *Part. Part. Syst. Characterisation*, **17**, 146-158, 184
- 149 Blandin, A-F, Rivoire, A., Mangin, D., Klein, J-P. and Bossoutrot, J-M. (2000), *Part. Part. Syst. Charact.*, **17**(1) 16-20, 184
- 150 Watano, S. and Sparks, R. (1995), *Powder Technol.*, **83**, 55-60, 185
- 151 HogeKamp, S., Fakouhl, N. and Schubert, H. (1995), *4th Internatioonal Congr. Optical Particle Sizing*, Preprints 553-562, Partec, Nürnberg, Grmany, publ. NürnbergMesse, GmbH, 185
- 152 Schmidt, F., Schmidt, K.G. and Fissan, H. (1991), *Reinraumtechnik*, **1**, 38-39, 186
- 153 Schmidt, F., Dickens, J. and Fissan, H. (1998), *Partec 98, 7th European Symp. Particle Charact.*, 685-694, Nürnberg, Germany, publ. NürnbergMesse GmbH, 186
- 154 Mang, J.T., Skidmore, C.B., Kramer, J.F. and Phillips, D.S. (2000), *Int. Annu. Conf. ICT, 31st (Energetic Materials)*, 20/1-20/8, 186
- 155 Astrakharchik-Farrimond, E., Shekunov, B.Y., Sawyer, N.B.E., Morgan, S.P., Somekh, M.G. and See, C.W. (2003), *Part. Part. Syst. Charact.*, **20**, 104-110, 187
- 156 Jillavenkatesa, A., Dapkunas, S.J. and Lum, L-S, H. 2001, Particle Size Characterization, *National Institute of Standards and Trchnology, Sp. Publ.* 960-1, 188
- 157 Kay, D.H. (1965), *Techniques for Electron Microscopy*, 2nd ed., Blackwell Scientific, Publ. Oxford, U.K., 188, 191, 192

206 Powder sampling and particle size determination

- 158 Lange, H. (1995), *Part. Part. Syst. Charact.*, **12**, 148-157, 188
- 159 Drummond, D.G., (1950), *The Practice of Electron Microscopy*, Royal Microscopy Society, London, 189, 190
- 160 Walton, W.H. (1947), *Trans. Inst. Chem. Engrs.*, suppl. **25**, 64-76, 189, 190, 192
- 161 Cartwright, J. and Skidmore, J.W. (1953), Rep. No. 79, *Safety in Mines Res. Est.*, Sheffield, U.K., 190
- 162 Revell, R.S.M. and Agar, A.W. (1955), *Brit. J. Appl. Phys.*, **6**, 23, 190
- 163 Bradley, D.E. (1954), *Brit. J. Appl. Phys.*, **5**, 65, 190
- 164 Backus, R.C. and Williams, R.C. (1956), *Br. J. Appl. Phys.*, **21**, 11, 191
- 165 Hamilton, R.J. and Phelps, B.A. (1956), *Brit. J. Appl. Phys.*, **7**, 186, 191
- 166 Cartwright, J. and Skidmore, J.W. (1953), Rep. No. 79, *Safety in Mines Res. Est.*, Sheffield, U.K., 191
- 167 Joffe, A.D. (1963), *Brit. J. Appl. Phys.*, **14**(7), 429, 191
- 168 Chu, Y.F. and Ruckenstein, E. (1976), *J. Catalysis*, **41**(3), 373-383, 191
- 169 Ruzek, J. and Zbuzek, B. (1975), *Silikaty*, **19**(1), 49-66, 191
- 170 Anderson, R., Tracy, B. and Bravman, J. (1992), *Mat. Res. Soc.*, **254**, 191
- 171 Bradley, D.E. and Williams, D.J. (1957), *J. Gen. Microbiology*, **17**, 75, 192
- 172 Bailey, G.W. and Ellis, J.R. (1954), *Microscope*, **14**(6), 217, 192
- 173 Concoran, J.F. (1970), *Fuel*, **49**(3), 331-334, 192
- 174 Eckert, J.J.D. and Caveney, R.J. (1970), *Brit. J. Appl. Phys. E*, 423-414, 192
- 175 Williams, R.C. and Wyckoff, R.W.G. (1946), *Br. J. Appl. Phys.*, **17**(23), 192
- 176 Chang, C.C. (1971), *Surface Sci.*, **25**, 23, 192
- 177 Taylor, N.J. (1969), *PhD thesis*, London Univ., U.K., 192
- 178 Brundle, C.R. (1972), *Surface and Defect Properties of Solids*, ch. 6, Chem. Soc., London, U.K., 193
- 179 Szalkowski, F.J. (1977), *J. Colloid Interf. Sci.*, **58**(2), 199-215, 193
- 180 Hay, W. and Sandberg, P. (1967), *Micropaleontology*, **13**, 407-418, 193
- 181 McCarthy, J.J. and Ferrara, P.R. (1982), *Microbeam Analysis*, 118-120, 193
- 182 Petruk, W. (1988), *Scanning Microsc.*, **2**, 1247-1256, 194
- 183 Kolendik, O. (1981), *Practical Metallogr.*, **18**, 562-573, 194
- 184 Kramarenko, I.B. (1985), *Probl. Proch.*, **3**, 84-87, 194
- 185 Shoji, T., Okaya, K., Goto, K. and Otsukia, S. (1987), *Fine Particle Soc. Mtng.*, Boston., 194
- 186 ASTM E766-98, Standard Practice for Calibrating the Magnification of a Scanning Electron Microscope, 194
- 187 Morton R.R.A. and Martens, A.E. (1972), *Res. Dev.*, **23**(1), 24-26, 28, 194
- 188 Morton, R.R.A. (1972), Measurement and Analysis of Electron Beam Microscope Images, Form 7050, Bausch & Lomb, 194
- 189 McCarthy, J.J. and Benson, J.P. (1984), *Form No Xr2112A*, Tracor Northern, 194
- 190 McCarthy, J.J., Fisher, R.M. and Lee, R.J. (1982), *Ultramicroscopy*, **8**, 351-360, 194
- 191 Krinsley, D. and Margolis, S. (1969), *Trans. N.Y. Acad. Sci.*, **31**, 457-477, 194

- 192 Turner, G.A., Fayed, E. and Zackariah, K. (1972), *Powder Technol.*, **6**, 33-37, 194, 195
- 193 Willard, R.J. and Hjelmstad, K. E. (1969/70), *Powder Technol.*, **3**, 311-313, 194
- 194 White, E.W. *et al.* (1970), Proc. 3rd Ann. SEM Symp., *Illinois Inst. Technol.*
- 195 King, R.P. and Schneider, C.I. (1993), *Kona, Powder and Particle*, No 11, Council of Powder Testing, Japan, pp 165-178, 195
- 196 Kocova, S., Thibert, R. and Tawashi, R. (1993), *J. Pharm. Sci.*, **82**, 844, 195
- 197 Fini, A., Fernandez, M.J., Holgado, M.A. and Rabasco, A.M. (1998), *Proc 1st European Symp. Process Technol. in Pharmaceutical Sci.*, Nürnberg, Germany, publ. NürnbergMesse GmbH. MesseZentrum, Germany, 195
- 198 Sarid, D. (1992), *Scanning Force Microscopy with Applications to Electric, Magnetic and Atomic Forces*, Oxford Univ. Press, .N.Y., 195
- 199 Binnig, G., Rossiter, B.W. and Hamilton, J.F. (1981), *Eur. Pat. Appl.* 27517, 196
- 200 Binnig, G., Rohrer, H., Gerber, C.H. and Weibel, E. (1982), *Phys. Rev. Letters*, **49**, 57, 196
- 201 Scott D.M. (2002), *World Congress on Particle Technology WCPT4*, Australia ., 196
- 202 Vaz, C.M.P., Herrmann, P.S.P. and Crestana, S. (2002), *Powder Technol.*, **126**, 21-58, 196
- 203 Lee, W.P., Snow, W.S., You, H.K. and Tou, T.Y. (2001), *Japan J. Appl. Physics, Part I*, **40**(1), 18-23, 196
- 204 Junno, T., Anand, S., Deppert, K., Montelius, L. and Samuelson, H. (1995), *Appl. Phys. Letters*, **66**, 3295, 3627, 199
- 205 Schleicher, B., Jung, T. and Burtscher, H. (1993), *J. Colloid Interf. Sci.*, **16**, 277, 199
- 206 Kütz. S. and Schmidt-Ott, A. (1990), *J. Aerosol Sci.*, **21**, S47, 199
- 207 Schmidt-Ott, A., Marson, B. and Sattler, K. (1997), *J. Aerosol Sci.*, **28**, S729, 199
- 208 Wiesendanger, R. and Güntheradt, H.J. (1992), *Scanning Tunneling Microscope, I and II*, pp246 and 308 resp., Springer Series in Surface Science, #21 and #28, Springer Verlag, N.Y., 199
- 209 VazPaulo, C.M.P., Hermann, S.P. and Crestana, S. (2002), *Powder Technol.*, **126**(1), 51-58, 199
- 210 Zeng, R. and Rand, B. (2000), *J. Wuhan Univ. Technol. Mater. Sci., ed.*, **15**(2), 7-14, 200